

# Pathological Mechanisms of Radiation-Induced Lung Injury and Novel Nano-Drug Delivery Therapeutic Strategies

Xiaohuo Zhang<sup>1,\*</sup>, Zhiruo Zhang<sup>2</sup>, Mi Huang<sup>2</sup>, Yufan Jin<sup>2</sup>, Youming Huang<sup>2</sup>, Peng Ji<sup>1,2,3,\*</sup>, Zhenchao Ma<sup>1,\*</sup>

<sup>1</sup>Huzhou Central Hospital, Fifth School of Clinical Medicine of Zhejiang Chinese Medical University, Huzhou, Zhejiang, 313000, People's Republic of China; <sup>2</sup>School of Pharmacy, Taizhou University, Taizhou, Jiangsu, 225300, People's Republic of China; <sup>3</sup>Liangzhu Laboratory, Zhejiang University School of Medicine, Hangzhou, Zhejiang, 310000, People's Republic of China

\*These authors contributed equally to this work

Correspondence: Peng Ji, School of Pharmacy, Taizhou University, No. 93, Jichuan East Road, Taizhou, Jiangsu, 225300, People's Republic of China, Email jipeng0213@163.com; Zhenchao Ma, Huzhou Central Hospital, Fifth School of Clinical Medicine of Zhejiang Chinese Medical University, No. 1558 North Sanhuan Road, Huzhou, Zhejiang, 313000, People's Republic of China, Email mazhenchao@hzhospital.com

**Abstract:** Radiation-induced lung injury (RILI), encompassing early radiation pneumonitis (RP) and late radiation-induced lung fibrosis (RILF), remains a major dose-limiting complication of thoracic radiotherapy. The pathological processes involve oxidative stress, DNA damage, inflammatory cascades (notably IL-1, IL-6, TNF- $\alpha$ , and TGF- $\beta$ ), and fibrotic remodeling, yet current therapies—such as corticosteroids and antifibrotic agents—provide only partial relief and are often accompanied by significant side effects. Recent advances in nano-drug delivery systems (NDDS) offer new opportunities to overcome these limitations through targeted pulmonary delivery, stimuli-responsive release, and synergistic modulation of pathological pathways. Nanoformulations, including hyaluronic acid-based carriers, ROS-responsive microspheres, and inhalable nanomedicines, demonstrate enhanced pulmonary bioavailability, reduced systemic toxicity, and multi-mechanistic therapeutic potential. With continued refinement of intelligent nanocarriers and integration of advanced diagnostic tools, NDDS holds strong promise for translating preclinical advances into precise, individualized therapies for RILI.

**Keywords:** radiation pneumonitis, radiation-induced lung injury, nano-drug delivery system, stimuli-responsive release, targeted drug delivery, lung-targeted nanomedicine

## Introduction

Radiation-induced lung injury (RILI) represents one of the most prevalent non-malignant complications associated with thoracic radiotherapy for malignant tumors, predominantly involving normal lung parenchyma within the irradiated field.<sup>1,2</sup> RILI is characterized by a biphasic pathological progression, encompassing an acute inflammatory phase and a chronic fibrotic phase. The acute phase, commonly referred to as radiation pneumonitis (RP), typically manifests within six months following radiotherapy and is marked by an inflammatory response in the pulmonary tissue. In contrast, the late phase, known as radiation-induced lung fibrosis (RILF), generally emerges beyond six months post-irradiation and is defined by irreversible fibrotic remodeling and persistent scarring of the lung architecture.<sup>3,4</sup>

RP is an immune-mediated inflammatory response triggered by irradiation of adjacent normal lung parenchyma during thoracic radiotherapy.<sup>1,5</sup> Histopathologically, RP is characterized by infiltration of inflammatory cells, injury to alveolar epithelial and vascular endothelial cells, and disruption of ventilation–perfusion balance.<sup>6</sup> The inflammatory cascade involves multiple cytokines—most prominently IL-1, IL-6, TNF- $\alpha$ , and TGF- $\beta$ —which modulate apoptosis, fibrotic signaling, and tissue repair. These mediators constitute the major drivers of RP pathogenesis, ensuring consistency with current evidence. As such, RP constitutes a clinically significant complication of thoracic radiotherapy.<sup>2</sup> Its incidence is modulated by a combination of patient-related factors—such as age, sex, smoking history, comorbidities, tumor type, and anatomical location—and treatment-related parameters, including total radiation dose, fractionation

scheme, irradiated lung volume, and the use of concurrent chemotherapy or immunotherapy.<sup>3,7,8</sup> Furthermore, inter-individual variability in biological responses contributes to the unpredictable nature of RILI risk.

RILI remains a significant dose-limiting toxicity in thoracic radiotherapy, even as its incidence has declined with the adoption of advanced techniques such as three-dimensional conformal radiotherapy, intensity-modulated radiotherapy (IMRT), and stereotactic body radiotherapy (SBRT).<sup>9,10</sup> It poses significant challenges to treatment efficacy and continues to adversely affect patient quality of life.<sup>11,12</sup> RP, a hallmark manifestation of RILI, is typically identified on radiographic imaging by interstitial infiltrates and ill-defined pulmonary consolidations. In severe cases, RP may progress to acute respiratory distress syndrome (ARDS). The condition is often characterized by an insidious onset and rapid clinical deterioration, contributing to its high morbidity and mortality rates.<sup>13</sup>

This review provides a comprehensive overview of the pathogenesis and recent diagnostic advances related to RILI, encompassing both RP and RILF. Particular emphasis is placed on emerging insights into cellular injury mechanisms, the activation of inflammatory signaling pathways, and the role of immune modulation. Furthermore, the review examines the therapeutic potential of NDDS in the prevention and management of RP, highlighting recent innovations that enhance therapeutic timing, improve pharmacological efficacy, and minimize systemic toxicity through the targeted delivery of anti-inflammatory and anti-fibrotic agents. By bridging basic research and clinical application, this review aims to offer novel perspectives and future directions for the precise diagnosis and individualized treatment of RP.

In the context of RILI, NDDS present distinct advantages over emerging therapeutic strategies such as cell therapy and immunomodulation. Unlike cell therapy, NDDS enables site-specific drug release through targeted delivery and stimulus-responsive mechanisms,<sup>14</sup> thereby enhancing therapeutic stability, minimizing systemic toxicity, and potentially acting synergistically with cellular approaches to improve efficacy. Compared with immunomodulators, NDDS can increase bioavailability, mitigate adverse effects,<sup>15</sup> and facilitate multi-target regulation. Significantly, NDDS has already progressed into clinical evaluation for pulmonary diseases. For example, inhalable liposomal formulations of nintedanib and miR-302 nanoparticle inhalation systems have demonstrated favorable safety and efficacy in pulmonary fibrosis, while budesonide nanosuspensions have yielded promising outcomes in pulmonary infection and inflammation. Although the application of NDDS in RILI remains at an exploratory stage, accumulating preclinical evidence has established a solid foundation for translation, accelerating the trajectory from experimental validation to clinical application.

## Pathophysiology and Mechanisms of RP

### Radiation Lung Injury

RT is a cornerstone treatment modality for patients with medically inoperable malignancies or locally advanced tumors deemed unsuitable for surgical resection.<sup>16</sup> However, RILI remains a principal dose-limiting complication in thoracic radiotherapy, with its reported incidence varying due to inconsistent clinical definitions and diagnostic criteria.<sup>3</sup> RILI may occur in individuals receiving total body irradiation as part of hematopoietic stem cell transplantation protocols, as well as in patients undergoing localized thoracic irradiation for malignancies such as breast cancer, lung cancer, and lymphoma. RILI exhibits distinct temporal phases, progressing from early-stage RP, typically developing within six months post-irradiation, to late-stage RILF, emerging beyond six months. Both phases involve a complex cascade of pathophysiological events, including epithelial and endothelial cell injury, inflammatory cell infiltration, cytokine release, fibroblast activation and differentiation, extracellular matrix (ECM) accumulation, and excessive collagen deposition. These processes culminate in characteristic radiographic findings and nonspecific clinical symptoms such as cough, fatigue, dyspnea, fever, and imaging abnormalities. Given the multifactorial nature and clinical impact of RILI, advancing strategies for its prevention and management remains a critical priority. Over the past decades, substantial progress has been made in elucidating the influence of radiation dose parameters and radiomic biomarkers on RILI risk.<sup>17,18</sup> More recently, the integration of novel therapeutic modalities—including molecularly targeted agents and immune checkpoint inhibitors—into radiotherapeutic regimens has introduced additional complexity to the underlying pathogenesis. Specifically, ICIs may amplify T-cell activation in irradiated lung tissues, exacerbating inflammatory cascades via increased secretion of pro-inflammatory cytokines (eg, IFN- $\gamma$ , TNF- $\alpha$ ) and promoting immune cell infiltration, which further complicates the molecular mechanisms and progression of RILI.<sup>19,20</sup>

## Cellular and Molecular Mechanisms

RP is predominantly initiated by oxidative stress and radiation-induced DNA damage (Figure 1). Redox homeostasis serves as a critical defense mechanism against various exogenous insults, including viral infections. However, prolonged exposure of cells to highly reactive oxidative species—both free radicals (eg, hydroxyl radical,  $\cdot\text{OH}$ ) and non-radical species (eg, hydrogen peroxide,  $\text{H}_2\text{O}_2$ )—can disrupt this balance, leading to oxidative stress. This pathological state arises either from excessive production of reactive oxygen species (ROS) and reactive nitrogen species (RNS) or from impairment of the endogenous antioxidant defense system.<sup>21,22</sup> Both exogenous and endogenous mechanisms drive ROS generation. Exogenous sources include environmental exposures such as cigarette smoke, secondhand smoke, heavy metals, air pollutants, and ionizing radiation. Endogenously, ROS may be produced by activated inflammatory cells (eg, epithelial cells and alveolar macrophages), the mitochondrial electron transport chain, and intracellular oxidase enzymes.<sup>23</sup> Due to their high reactivity and chemical instability,<sup>24</sup> ROS can inflict significant cellular damage if not neutralized. The body employs a multifaceted antioxidant defense system comprising enzymatic antioxidants—including superoxide dismutase (SOD), glutathione peroxidase (GPx), and catalase (CAT)—as well as non-enzymatic antioxidants such as albumin, mucin, and dietary constituents (eg, vitamin C [ascorbic acid], vitamin E [tocopherol], carotenoids, and flavonoids), which collectively act to mitigate ROS-induced oxidative injury.<sup>25</sup>

Ionizing radiation induces direct physical damage to DNA, including base loss, single-strand breaks (SSBs), and double-strand breaks (DSBs).<sup>29</sup> Although endogenous DNA repair mechanisms can partially mitigate such damage,

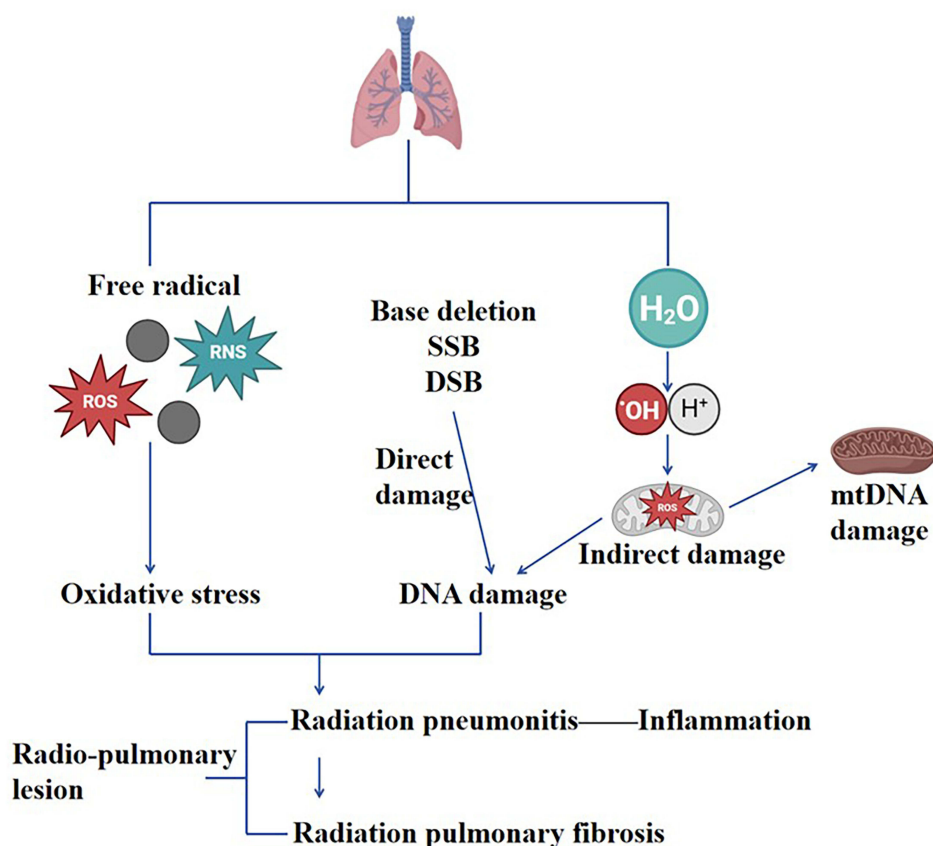


**Figure 1** Schematic diagram of the mechanisms by which oxidative stress and DNA damage contribute to the pathogenesis of RP. Ionizing radiation directly or indirectly (through radiolysis of water molecules, which generates ROS) causes DNA damage (such as base loss, single-strand breaks (SSBs), and double-strand breaks (DSBs)) and oxidative stress. Excessive ROS induces mitochondrial damage (including mtDNA), protein carbonylation, lipid peroxidation, and activates key signaling pathways (such as TGF- $\beta$ , PDGF, and IL-1-mediated pathways), collectively promoting inflammatory responses and lung tissue damage. These pathways have been mechanistically linked to radiation-induced lung injury in prior studies: Weber A, Wasiliew P, Kracht M. Interleukin-1 (IL-1) pathway[J]. *Science signaling*, 2010, 3(105): cm1.<sup>26</sup> Bonner J C. Regulation of PDGF and its receptors in fibrotic diseases[J]. *Cytokine & growth factor reviews*, 2004, 15(4): 255–273.<sup>27</sup> McCartney-Francis N L, Frazier-Jessen M, Wahl S M. TGF- $\beta$ : a balancing act[J]. *International reviews of immunology*, 1998, 16(5–6): 553–580.<sup>28</sup>

residual lesions may still lead to apoptosis or genomic mutations. In addition to direct effects, ionizing radiation also generates ROS, primarily through the ionization of intracellular water molecules, resulting in indirect DNA damage and further exacerbating structural disruption.<sup>25,30</sup> The deleterious effects of ROS are not confined to mitochondrial DNA (mtDNA) injury; ROS also initiates a cascade of cellular responses, including protein carbonylation, membrane lipid peroxidation, heightened oxidative metabolism, accumulation of spontaneous mutations, and an increased risk of malignant transformation.<sup>31</sup> Importantly, DNA damage and ROS production exhibit synergistic interactions, co-regulating several key signaling pathways implicated in radiation-induced tissue injury, such as TGF- $\beta$ -mediated fibrotic signaling, PDGF-driven cellular proliferation, and IL-1-associated inflammatory responses.<sup>32</sup>

## The Role of Inflammatory Responses and Key Mechanisms in the Development of RP

The pathogenesis of RP involves the release of damage-associated molecular patterns (DAMPs), which serve as danger signals that recruit various immune cells to sites of injury, thereby exacerbating pulmonary tissue damage and promoting tissue remodeling.<sup>18</sup> DAMPs mediate the upregulation of intercellular adhesion molecule-1 (ICAM-1) and platelet endothelial cell adhesion molecule-1 (PECAM-1/CD31), facilitating the migration of neutrophils and macrophages into the irradiated lung tissue. These infiltrating immune cells subsequently release pro-inflammatory cytokines, including interleukin-6 (IL-6), tumor necrosis factor- $\alpha$  (TNF- $\alpha$ ), and TGF- $\beta$ , which contribute to the amplification of local inflammatory responses.<sup>18,33–35</sup>

Lymphocytes play a pivotal role in the acute phase of radiation-induced pneumonitis.<sup>18,36</sup> T helper 1 (Th1) cells secrete interferon-gamma (IFN- $\gamma$ ), which activates the JAK-STAT1 signaling pathway within phagocytes, thereby promoting the polarization of macrophages toward the pro-inflammatory M1 phenotype. These M1 macrophages release inflammatory mediators such as interleukin-2 (IL-2) and nitric oxide (NO), contributing to the amplification of the inflammatory response.<sup>37,38</sup> While Th1 cells are generally associated with anti-fibrotic effects, T helper 2 (Th2) cells promote fibrosis through the secretion of interleukin-4 (IL-4) and interleukin-13 (IL-13), which activate the TGF- $\beta$ /Smad signaling pathway. This cascade facilitates fibroblast activation and collagen synthesis, thereby promoting the development of pulmonary fibrosis.<sup>39–41</sup>

An imbalance in Th1/Th2 responses is a key driving mechanism in the persistent progression of RP.<sup>39,40</sup> Regulatory T cells (Tregs), through the expression of pro-inflammatory chemokine receptors such as CCR2, CCR4, and CCR5, can amplify inflammatory responses, promote epithelial–mesenchymal transition (EMT), and suppress Th17-mediated immunity, thereby exacerbating structural damage to pulmonary tissue.<sup>42</sup> Emerging evidence also suggests that immune checkpoint inhibitors (ICIs) can intensify T-cell activation and immune responses, contributing significantly to the onset and severity of RP.<sup>43–45</sup>

TGF- $\beta$  serves as a critical molecular link between RP and RILF, promoting fibroblast activation and collagen synthesis and playing a central role in the fibrotic process.<sup>46</sup> Interferon-gamma (IFN- $\gamma$ ), conversely, exerts anti-fibrotic effects by inhibiting TGF- $\beta$ -induced Smad3 phosphorylation.<sup>47</sup> Recent studies have also identified gastrin-releasing peptide (GRP) as a novel mediator in the inflammation-to-fibrosis transition. Inhibition of GRP signaling has been shown to significantly reduce macrophage infiltration and collagen deposition, suggesting its potential as a therapeutic target to prevent the progression of RP to RILF.<sup>48,49</sup>

In addition to TGF- $\beta$ , platelet-derived growth factor (PDGF) represents a critical mediator in the progression of RILF, particularly in the fibrotic phase.<sup>18</sup> Among its isoforms, PDGF-BB has been identified as a potent mitogenic and chemotactic factor for fibroblasts and myofibroblasts. Post-irradiation, PDGF is predominantly released by activated macrophages and platelets at sites of microvascular damage, with injured epithelial and endothelial cells also contributing to its local abundance. Upon binding to its cognate receptor (PDGFR) on fibroblasts, PDGF initiates downstream signaling cascades—most notably the phosphoinositide 3-kinase/protein kinase B (PI3K/Akt) and mitogen-activated protein kinase (MAPK) pathways—that facilitate fibroblast proliferation, migration, and resistance to apoptosis.<sup>50</sup> Persistent activation of these pathways fosters the accumulation of fibroblasts. It promotes excessive ECM deposition, particularly of collagen, thereby facilitating the transition from inflammatory RP to irreversible fibrotic remodeling characteristic of RILF.<sup>51–53</sup>

Collectively, the inflammatory response in RP is orchestrated by a complex network of immune cells, cytokines, and signaling pathways. This intricate immunological landscape presents a broad array of potential therapeutic targets for the management and treatment of RP.

## The Continuum of Pathogenesis Between Radiation Pneumonitis and Radiation-Induced Lung Fibrosis: Key Transitional Factors

RP and RILF represent temporally distinct but pathophysiologically interconnected stages of RILI, forming a dynamic continuum rather than isolated clinical entities. Together, they constitute the progressive pathological trajectory of RILI, involving multiple phases, diverse cellular populations, and complex signaling networks.<sup>3</sup> In the early phase of radiation exposure, direct injury to alveolar epithelial and vascular endothelial cells results in cell death and the release of damage-associated molecular patterns (DAMPs), which initiate innate immune activation. This is accompanied by the infiltration of inflammatory cells, including neutrophils, macrophages, and lymphocytes, and the release of pro-inflammatory cytokines such as interleukin (IL)-1, TNF- $\alpha$ , and IL-6. Concurrently, oxidative stress and DNA damage activate NADPH oxidase complexes and trigger ROS-associated signaling cascades, including p38 MAPK and NF- $\kappa$ B pathways. These processes markedly upregulate the transcription and secretion of TGF- $\beta$ , a key driver of the transition from inflammation to fibrosis.<sup>54</sup> Clinically, this phase is manifested as acute RP, with nonspecific symptoms such as dry cough, dyspnea, and low-grade fever.

If inflammation persists or immune regulation becomes dysregulated, reparative processes shift toward pathological remodeling. Sustained activation of the ROS–TGF- $\beta$  axis promotes the differentiation of fibroblasts into myofibroblasts, resulting in excessive synthesis and deposition of ECM components, particularly collagen.<sup>54</sup> Although interferon-gamma (IFN- $\gamma$ ) may inhibit TGF- $\beta$ /Smad3 phosphorylation and exert anti-fibrotic effects, factors such as Th1/Th2 imbalance, regulatory T cell (Treg) accumulation, and enhanced epithelial–mesenchymal transition (EMT) further facilitate the progression from RP to RILF. Mechanistically, TGF- $\beta$  binds to its type I and II receptors, inducing phosphorylation of Smad2/3. These phosphorylated Smads complex with Smad4 and translocate to the nucleus, where they regulate the transcription of fibrosis-related genes. Negative feedback is mediated by Smad7, while non-canonical pathways, including MAPK and ERK signaling, act synergistically to promote ECM production.<sup>55,56</sup>

Gastrin-releasing peptide (GRP), recently identified as a critical mediator bridging inflammation and fibrosis, has been implicated in this cascade. Elevated GRP levels are closely associated with TGF- $\beta$  activation, macrophage infiltration, and collagen accumulation. Notably, GRP inhibition has been shown to significantly attenuate fibrotic progression, highlighting its potential as a therapeutic target.<sup>57</sup> At the tissue level, RILF is characterized by alveolar wall thickening, reduced pulmonary compliance, and impaired gas exchange, ultimately culminating in irreversible structural changes such as honeycomb lung and progressive loss of lung function. As the disease advances, patients may experience severe complications including chronic respiratory failure, pneumothorax, malnutrition, and weight loss.

The transition from RP to RILF represents a pathological “rebalancing” from inflammation-dominant to fibrosis-dominant states, orchestrated by key regulatory elements such as the ROS–TGF- $\beta$  signaling axis, GRP activity, Th1/Th2 cytokine dynamics, and immune cell lineage shifts.<sup>58</sup> Therefore, early identification and targeted intervention within this molecular cascade—particularly through inhibition of ROS-mediated TGF- $\beta$  activation—are critical strategies to prevent fibrotic progression and improve long-term outcomes in patients with RILI.

## Clinical Manifestations and Diagnostic Procedures

Based on the complex pathophysiological mechanisms of RP described above, patients undergoing thoracic radiotherapy present with specific clinical manifestations that need to be recognized and evaluated with the help of multiple diagnostic tools. The clinical manifestations of RP are varied and lack specificity, and its diagnosis requires a combination of history, symptoms, signs, and auxiliary findings. The clinical presentation features of RILI and the primary current diagnostic methods will be systematically described below.

## Clinical Manifestations

RILI includes early-stage RP, late-stage RILF. The alveolar capillary barrier in the lungs, which is very sensitive to ionizing radiation, is exposed to ionizing radiation, which immediately causes oxidative damage to cellular macromolecules such as nuclear DNA and Mitochondria, generates free radicals, and causes type I lung cells and vascular endothelial cells to undergo cytotoxic damage and activate the cell signaling cascade.<sup>1,11</sup> These damages activate a multidimensional DNA damage response within a few hours, the outcome of which depends on several factors such as the dose of radiation, the mode of exposure, the type of exposure, the extent and nature of the DNA damage, etc, and leads mainly to a transient arrest of the cell cycle.<sup>59</sup> The signaling cascade of damaged cells releases pro-inflammatory cytokines, so infiltrated immune cells, including immune cells such as inflammatory monocytes and lymphocytes, are observed within hours to days of irradiation to accomplish tissue repair and protection. However, most immune cells are highly radiosensitive, and acute death occurs with low-dose irradiation, causing a transient early decline in resident alveolar macrophages and blood lymphocytes.<sup>60</sup> At the same time, radiation exposure activates inhibitory immune signaling, upregulation of the PD-1/PD-L1 pathway suppresses T-cell activity, natural killer (NK) cell cytotoxicity is inhibited, suppressing local immune responses, and more extended periods of radiation cause pro-inflammatory factors to accumulate and shift to an inhibitory environment, which also suppresses immune cell activation and exacerbates inflammatory responses. At 3–12 weeks of radiotherapy, radiation has extensively damaged epithelial and endothelial cells, leading to alveolar collapse, formation of pulmonary capillary stenosis, and microvascular thrombosis.<sup>1,61</sup> Based on these pathophysiologic mechanisms, patients usually present with dyspnea and dry cough in the early stages (see Figure 2). In addition, less common clinical features of RP include hemoptysis, airway obstruction, pulmonary vascular injury, bronchitis, respiratory infections, pleural effusion, and pneumothorax. If early treatment is not effective, there is a high probability of transformation to RILF, with symptoms such

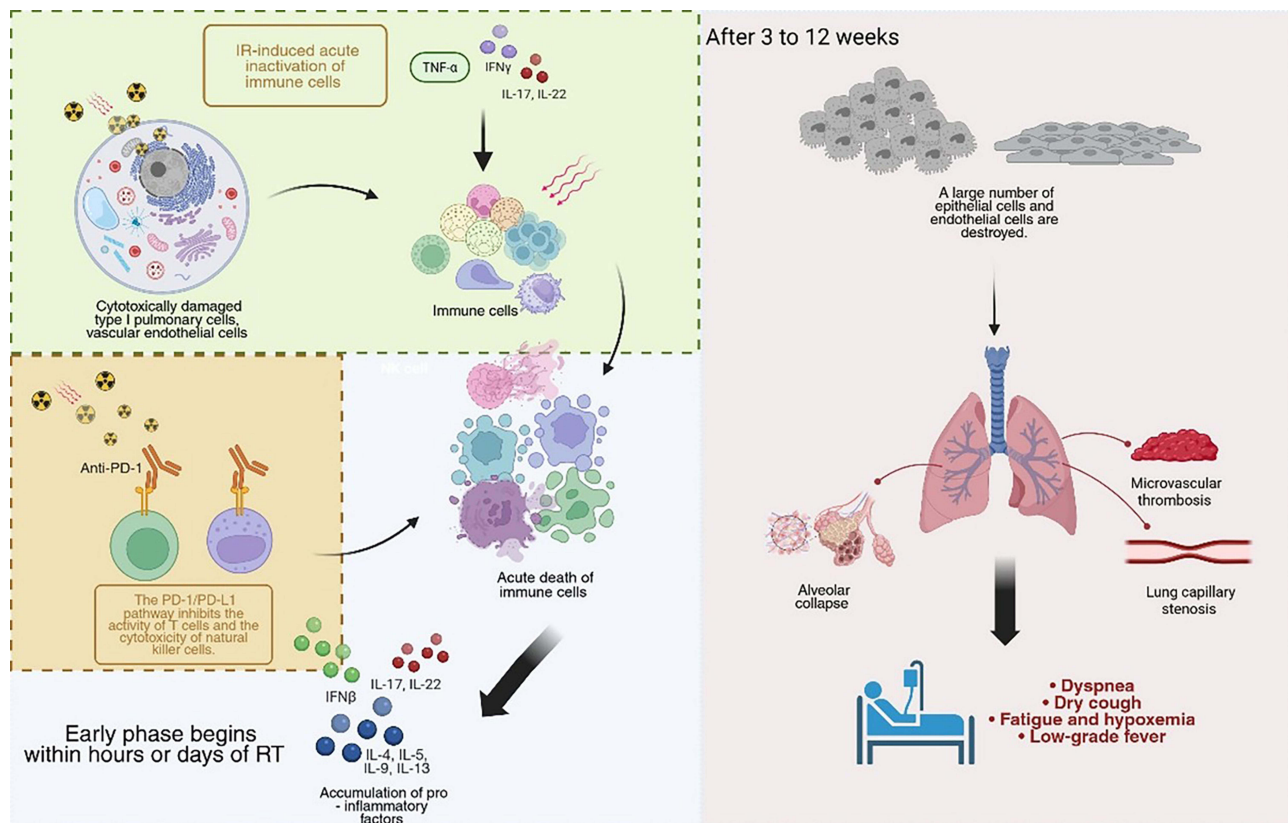


**Figure 2** Schematic diagram of the pathophysiologic mechanisms of RP. Ionizing radiation damages alveolar epithelial cells (type I, type II) and vascular endothelial cells, leading to disruption of the alveolar capillary barrier. Injured cells release DAMPs and pro-inflammatory cytokines (eg, TNF- $\alpha$ , IL-1, IL-6, TGF- $\beta$ ), which recruit and activate inflammatory cell infiltrates such as neutrophils, macrophages, and lymphocytes. A sustained inflammatory response, oxidative stress, and the driving of key factors (eg, TGF- $\beta$ ) may ultimately lead to fibroblast activation and proliferation, myofibroblast transformation, and excessive deposition of ECM, culminating in radiation-induced lung fibrosis (RILF).

as shortness of breath, cyanosis, chest pain, and wet rales or pleural friction on chest auscultation.<sup>1</sup> However, the diversity and atypicality of these acute-phase symptoms are similar to those of other lung diseases, which increases the difficulty of early diagnosis; therefore, clinical diagnosis needs to be closely combined with the history of radiotherapy and imaging examinations to make a comprehensive judgment.

## Diagnostic Procedures

### X-Ray Examination

Chest X-rays are commonly used as a preliminary test in the diagnosis of RILI because they are highly coincident with the irradiation field of the radiotherapy plan and have a regular rectangular, wedge, or polygonal distribution. In the early stages, the most common findings on chest radiographs are perivascular blurring, increased and disorganized lung texture, and the appearance of patchy or streaky shadows.<sup>62</sup> As for the chronic phase, as pulmonary fibrosis progresses, fibrous tissue proliferates and pulls on the lung tissues, leading to destruction of alveolar structure and contraction of lung tissues, and the lungs thus show lattice or honeycomb-like changes. However, the sensitivity of X-ray examination is relatively low, and the specificity is poor. Early RILI, which is characterized by mild inflammation of the alveoli and interstitium and has not yet caused significant changes in the density of lung tissue, is prone to misdiagnosis and misinterpretation. It cannot be clearly distinguished from lung infection and lung tumor metastasis.

### CT Examination

Chest CT, exceptionally high-resolution CT (HRCT), plays a vital role in the diagnosis of RILI and is an indispensable core diagnostic technique. The CT manifestations of RP are varied and include: diffuse ground-glass shadows, modified conventional type, mass-like solid lesions with volume reduction and tractional bronchiectasis, and scar-like changes; in the chronic phase, the CT images show changes specific to RILF, for example, the lung tissues show altered shapes such as striations, lattices, or honeycombs, as well as volume reduction, bronchiectasis, and distortion of the parenchymal structures and traction bronchodilatation, etc.<sup>63</sup> Based on its high resolution, CT examination can clearly show the details and the specific scope of lung lesions. Compared with X-ray examination, it is of great significance for the early detection of RILI, especially for some difficult-to-observe tiny lesions, as well as accurately evaluating the severity of the lesions, which will provide a key basis for the subsequent development of treatment programs.

### Pulmonary Function Tests

Pulmonary function tests are also one of the key steps in assessing the degree of lung function impairment in patients with RILI. In the early stages of the disease, lung function shows mild abnormalities, such as mild decreases in forceful lung volume (FVC), spirometry (VC), and diffusion of carbon monoxide (DLCO). Early RILI mainly interferes with the gas exchange process in the alveoli, resulting in a certain degree of impediment to gas intake and expulsion. However, it does not have a significant impact on the overall ventilation of the lungs.<sup>63</sup> With the progression of the disease, the lung function damage continues to increase, and fibrosis and inflammation occur in the lung tissues, leading to decreased lung elasticity and ventilation dysfunction. FVC and VC appear to be significantly decreased, and DLCO is further decreased, while residual volume of air (RV) and functional residual volume of air (FRC) may be increased as well.<sup>62</sup> The results of pulmonary function tests not only visualize the patient's current state of lung function, but can also be used to track the progression of the disease.

### Blood Tests

Blood-based biomarkers provide valuable adjunctive information for the diagnosis and assessment of RILI, particularly during the acute phase.<sup>64</sup> Common inflammatory indicators, including the neutrophil-to-lymphocyte ratio, white blood cell count, and C-reactive protein (CRP), are often elevated in response to radiation-induced pulmonary inflammation. As an acute-phase reactant, CRP is markedly upregulated in the early stages of RILI and reflects systemic inflammatory activity triggered by radiation-induced tissue damage.

In addition to general inflammatory markers, several cytokines have been identified as closely associated with the pathophysiology of RILI. Notably, elevated serum levels of TNF- $\alpha$ , TGF- $\beta$ , and interleukin-6 (IL-6) have been observed in patients with RILI.<sup>63</sup> TNF- $\alpha$ , primarily secreted by activated macrophages, plays a critical role in initiating inflammatory cascades by promoting endothelial activation, enhancing vascular permeability, and facilitating leukocyte extravasation into lung tissue. In contrast, TGF- $\beta$  serves as a central mediator in fibrogenesis, promoting fibroblast proliferation and stimulating the synthesis and deposition of ECM components such as collagen—hallmarks of radiation-induced pulmonary fibrosis.

Although individual biomarkers lack specificity for definitive diagnosis, serial monitoring of these parameters provides crucial adjunctive information for tracking inflammatory activity, assessing fibrotic progression, and evaluating therapeutic response over time. The diagnostic utility and limitations of each method are summarized in [Table 1](#).

## Histopathological Examination

While imaging modalities and clinical evaluation remain the primary approaches for diagnosing RILI, histopathological examination of lung tissue may be considered in cases with atypical clinical presentations or radiographic findings, diagnostic uncertainty, or when differentiation from other conditions—such as tumor recurrence or opportunistic infections—is required. Tissue acquisition methods include transbronchial lung biopsy (TBLB) via bronchoscopy or surgical lung biopsy through video-assisted thoracoscopic surgery (VATS) or open thoracotomy.<sup>71</sup> Histological evaluation enables direct visualization of alveolar architecture, interstitial changes, patterns of inflammatory cell infiltration, and the extent of fibrotic remodeling, thereby providing definitive diagnostic evidence. However, as an invasive procedure, lung biopsy carries inherent risks, such as hemorrhage and pneumothorax. It may yield false-negative results in the context of diffuse pulmonary involvement due to sampling limitations. Consequently, histopathological assessment is not routinely recommended for the diagnosis of RILI and should be reserved for selected cases with compelling clinical indications. A comprehensive diagnostic approach to RILI requires integration of multiple assessment modalities. Imaging techniques, including chest radiography for initial screening and high-resolution computed tomography (HRCT) as the diagnostic cornerstone, are essential for identifying characteristic pulmonary lesions. Pulmonary function tests provide quantitative evaluation of ventilatory and diffusion impairments, while circulating biomarkers—such as inflammatory mediators and cytokines—may assist in assessing the degree of inflammation and fibrotic activity. The diagnostic utility and limitations of each method are summarized in [Table 2](#).

## Treatment Strategies for RILI

### Current Treatment Strategies

According to the Global Cancer Statistics Report 2023,<sup>76</sup> the prevalence of RP in patients undergoing radiotherapy for thoracic tumors is as high as 30%. This data highlights the urgency and importance of research into its treatment strategies, and the severity of RP is usually categorized into five grades according to the CTCAE criteria (see [Table 3](#)).

### Glucocorticosteroid

Glucocorticoids are currently the most commonly used drugs to relieve the inflammatory response and associated symptoms in the acute phase of RP.<sup>77</sup> In the early phase of inflammation, it inhibits the activation and chemotaxis of inflammatory cells and reduces the release of inflammatory mediators, leading to a reduction in the symptoms of the alveolar and interstitial inflammatory response. In a study of RP patients, administration of glucocorticoid therapy significantly relieved symptoms such as cough and dyspnea, and lung inflammation was reduced. However, current evidence shows that glucocorticosteroids have limited reversal effects on advanced RILF, and long-term use may trigger adverse effects such as hyperglycemia, hypertension, increased risk of infection, and osteoporosis. In addition to this, some patients also suffer from varying degrees of immune suppression. Therefore, before the use of glucocorticoids, the patient's condition, physical status, and other iatrogenic factors need to be thoroughly evaluated to ensure that he or she meets the indications for the use of the drug.

**Table 1** Clinical Manifestations

Clinical Feature	Key Symptoms	Occurrence Frequency	Prevalence Data	Ref
Hemoptysis	Coughing up sputum with blood (which may present as blood streaks, blood clots, or whole mouthfuls of bright red blood). In severe cases, massive hemoptysis can occur, accompanied by symptoms such as coughing, chest pain, and dyspnea.	It is relatively rare and mostly occurs in the late stage of Radiation-Induced Lung Injury (RILI), when complications such as pulmonary fibrosis, combined with vascular injury, infection, or tumor progression, arise.	Currently, there is a lack of precise epidemiological data on RILI-associated hemoptysis. According to clinical observations, its incidence accounts for approximately 5% to 10% of RILI patients and is mostly associated with severe lung tissue damage.	[65]
Airway Obstruction	Dyspnea (either inspiratory or expiratory), wheezing, coughing, and expectoration (sputum may be thick and difficult to expectorate). In severe cases, cyanosis and tachypnea may occur, and lung function tests may show abnormal indicators of airflow limitation.	It has a moderate incidence rate and can occur in both the acute phase of RILI (where radiation pneumonitis causes airway mucosal edema and increased secretions) and the chronic phase (where pulmonary fibrosis leads to traction and compression of the airways by scar tissue).	Existing studies have shown that approximately 15% to 25% of RILI patients experience airway obstruction symptoms of varying degrees, among which obstruction caused by fibrosis in the chronic phase accounts for a higher proportion (about 60% to 70%).	[1]
Pulmonary Vascular Injury	In the early stage, there may be no obvious specific symptoms. As the injury worsens, dyspnea (prominent after activity), fatigue, and chest pain may occur. In severe cases, it can lead to pulmonary hypertension, manifested as lower extremity edema, jugular vein distention, and symptoms related to right heart insufficiency.	It has a high incidence rate and is one of the important pathological bases of RILI, persisting from the acute phase to the chronic phase. The acute phase is mainly characterized by vascular endothelial injury, while the chronic phase can progress to vascular remodeling.	Epidemiological data indicate that more than 80% of RILI patients have pathological changes of pulmonary vascular injury, among which approximately 20% to 30% will progress to clinically detectable pulmonary hypertension or vascular-related complications.	[66]
Bronchitis	Persistent cough (either dry cough or cough with mucous sputum), retrosternal discomfort or pain, increased sputum production (purulent sputum may appear when infected), and some patients may also have accompanying low-grade fever and fatigue.	It is relatively common and mostly occurs in the acute phase of RILI (resulting from radiation-induced inflammatory response of the bronchial mucosa), often accompanying radiation pneumonitis.	Clinical statistics show that the incidence of bronchitis in patients with acute RILI is approximately 30% to 45%, and the symptoms become more obvious when complicated with infection, with the incidence rate rising to more than 50%.	[67]
Respiratory Infections	Fever (body temperature may rise above 38.5°C), cough, expectoration of purulent sputum, sore throat, aggravated dyspnea, and some patients may also have accompanying systemic symptoms such as chills and myalgia.	It is a common complication. Due to lung tissue damage and decreased immune function, RILI patients are prone to secondary infections such as bacterial, viral, or fungal infections, which can occur in the acute phase or chronic phase.	According to literature reports, the incidence of respiratory tract infection in RILI patients is approximately 25% to 40%. Among them, in the chronic phase (pulmonary fibrosis stage), due to lung structure destruction and impaired clearance function, the incidence is significantly higher than that in the acute phase (about 25% to 30% in the acute phase and 35% to 40% in the chronic phase).	[68]

(Continued)

**Table I** (Continued).

Clinical Feature	Key Symptoms	Occurrence Frequency	Prevalence Data	Ref
Pleural Effusion	Dyspnea (worsening as the amount of effusion increases), chest pain (mostly dull or stabbing pain, aggravated by breathing or coughing), chest tightness, and fatigue. Physical examination shows decreased or absent breath sounds on the affected side, and imaging examinations reveal a fluid dark area in the thoracic cavity.	It has a moderate incidence rate, mostly occurring in the acute phase of RILI (caused by pleural effusion due to inflammation), and a few cases may occur in the chronic phase due to fibrosis, traction, and pleural adhesion.	Epidemiological studies show that the incidence of pleural effusion in RILI patients is approximately 10% to 20%. Among them, unilateral effusion accounts for about 70% to 80%, and the effusion volume is mostly small to moderate. The incidence of massive effusion is relatively low (about 1% to 3%).	[69]
Pneumothorax	Sudden chest pain (mostly stabbing or knife-like pain, with a short duration), dyspnea (severity related to the amount of pneumothorax and underlying lung function), and cough (mostly irritative dry cough). Some patients may experience restlessness and cyanosis (in cases of massive pneumothorax).	It is relatively rare, mostly occurring in the chronic phase of RILI when pulmonary fibrosis causes lung tissue rupture (formation and rupture of bullae), or in the acute phase when lung tissue necrosis and infection involve the pleura.	Currently, there is a paucity of epidemiological data on RILI-related pneumothorax. Clinical observations show that its incidence rate is approximately 2% to 5%, and it mostly occurs in patients with chronic pulmonary fibrosis, especially those complicated with bullae. The recurrence rate is about 10% to 15%.	[70]

**Table 2** Comparison of the Main Diagnostic Methods of RILI

Diagnostic methods	Typical performance	Advantages	Limitations	Ref
X-ray examination	Acute phase (RP): Increased and disorganized lung texture with striated or patchy shadows, typically confined to the irradiated field Chronic phase (RILF): Lattice or honeycomb changes in lung tissue, reduced lung volume	Easy and inexpensive to perform, it allows initial visualization of general lung lesions	Low sensitivity and poor specificity for early or mild RILI; poor visualization of lesion details; difficult to distinguish infection, metastasis, etc.	[62]
CT examination	Acute phase (RP): Ground glass-like changes (GGO), patchy solid shadows (modified conventional type, mass-like solid changes with volume loss and traction bronchiectasis, scar-like changes), often corresponding to the irradiated field Chronic phase (RILF): Striated, lattice, or honeycomb changes in lung tissue, lung volume reduction, bronchiectasis, traction bronchiectasis, and distortion of lung parenchymal structures	High resolution, high accuracy for RILI diagnosis and condition assessment; can clearly display lesion details and extent; provides a detailed basis for treatment planning	Relatively high cost; some radiation dose; not suitable for multiple examinations in a short time	[63]
Blood tests	Acute phase: elevated WBC count, neutrophil ratio, and CRP; elevated serum levels of TNF- $\alpha$ , TGF- $\beta$ , IL-6	Relatively easy to operate, good reproducibility; reflects systemic inflammatory state	Indicator changes lack specificity; other lung diseases or systemic inflammation cause similar changes; cannot be used alone for RILI diagnosis; serial monitoring may provide additional value	[63,64]
Pulmonary Function Tests	Early: mild decreases in VC, FVC, and DLCO Progressive phase: significant decrease in VC and FVC, further decrease in DLCO, possible increase in RV and FRC	Visualizes lung function status; valuable for assessing disease severity and progression	Results are highly dependent on patient cooperation; cannot specify the lung lesion nature; requires a combination with other tests	[62,63]
Pathological examination	Acute phase (RP): hyperplasia and swelling of alveolar epithelial cells, widened alveolar septa, congestion, edema, and inflammatory cell infiltration Chronic phase (RILF): thickened alveolar septa, massive collagen deposition, increased fibroblasts, destroyed alveolar structures, honeycomb lung formation	Defines lesion nature (inflammation/fibrosis) and extent; provides the most reliable histologic basis	Invasive procedure (risk of pneumothorax, hemorrhage); limited sampling representativeness (possible false-negatives); usually reserved for diagnostic uncertainty or research	[71]
Imaging histology/AI	Quantitative image feature prediction model based on radiomic features from planning CT and dose distribution	Noninvasive; early predictability of RILI risk and severity	Dependent on high-quality imaging data and standardized analysis, predictive models require validation in multi-center studies; routine clinical applications are still being explored	[72–75]

**Table 3** RP Grading Performance and Treatment

Grading	Manifestations	Treatment
Grade I	Patient is asymptomatic with imaging changes.	No medication is required; observation is sufficient.
Grade II	The patient's daily life (eg, cooking, shopping, etc) is limited, and symptoms such as fever, cough, and shortness of breath occur.	Without fever: Symptomatic treatment (antibiotics if indicated). Fever or CT scan showing acute exudative changes/neutrophil $\uparrow$ : Symptomatic treatment + antibiotics ( $\pm$ glucocorticoids).
Grade III	Severe symptoms, self-care limited (eg, dressing, eating), requiring oxygen therapy.	Glucocorticoids + antibiotics + symptomatic treatment, oxygen therapy if needed.
Grade IV	The patient's respiratory distress and its severity are life-threatening.	Glucocorticoids + antibiotics + symptomatic treatment + mechanical ventilation.
Grade V	Patient death	–

## Drug Interventions

### Antifibrotic Drugs

Pirfenidone is an antifibrotic drug that impedes the fibrotic process. In the treatment of RP, pirfenidone reduces collagen synthesis by inhibiting TGF- $\beta$  production, down-regulating the expression of pre-collagen I gene in the lungs, and lowering the hydroxyproline content in the lungs, thus alleviating pulmonary fibrosis.<sup>78</sup> Studies have shown that mice treated with pirfenidone have significantly reduced fibrosis in their lung tissues and improved lung function to some extent. However, there are some problems in the clinical application of pirfenidone, for example, some patients may have gastrointestinal reactions, skin rash, and other adverse reactions, affecting the use of the drug compliance.<sup>79</sup>

### Cytokine Modulators

Cytokines play a pivotal role in the development and progression of RP, so the development of therapeutic agents for RP targeting cytokine modulators has become a hot research topic. Since TGF- $\beta$  is favorable for the development of fibrosis in RP, an effective method for treating RP can be to inhibit the expression level of TGF- $\beta$  or to modulate its activity. Experimental studies have shown that intervention with TGF- $\beta$ -specific monoclonal antibodies can effectively inhibit the activation of the TGF- $\beta$  signaling pathway and significantly improve the pathological changes of pulmonary fibrosis in animal models. However, these therapeutic agents are currently limited to preclinical studies and have not yet been translated into the clinical setting, and their long-term therapeutic effects and potential adverse effects still need to be verified through large-scale clinical trials.<sup>80</sup>

### Chinese Medicine Treatment

Traditional Chinese medicine (TCM) has been explored as an adjunctive approach for RILI, mainly targeting inflammatory and fibrotic pathways. In the acute phase, certain herbal formulations (eg, Lung Cleansing and Detoxification Tang) were shown to reduce serum IL-6/TNF- $\alpha$  by inhibiting NF- $\kappa$ B signaling and to accelerate inflammatory absorption.<sup>81</sup> In the chronic phase, combinations such as Astragalus–Danshen attenuated TGF- $\beta$ /Smad3 signaling and improved lung diffusion capacity.<sup>82</sup> Meta-analyses further suggest that herbal interventions may reduce steroid-related side effects and improve adherence.<sup>83</sup> Different TCM intervention strategies and the distinction of their underlying data sources are detailed in Table 4. Nevertheless, current evidence supports TCM only as a supportive therapy, whereas NDDS-based interventions remain the focus of innovative strategies for RILI.<sup>84</sup>

### Radiotherapy Technology Optimization

The development of precision radiotherapy technology offers the possibility of reducing the risk of RP. Three-dimensional conformal radiotherapy (3D-CRT) and IMRT allow the shape of the high-dose area to be distributed in three dimensions to

**Table 4** Explanation of the Distinction of Data Sources Related to TCM Treatment for RILI

Data Type	Specific Data Content	Data Source Type	Basis & Explanation
Decreased Cytokine Levels	Qingfei Paidu Decoction (containing <i>Scutellaria baicalensis</i> and <i>Fritillaria ussuriensis</i> ) reduces serum IL-6/TNF- $\alpha$ levels by 45% through inhibiting the NF- $\kappa$ B pathway.	Preclinical model (animal experiment)	This study <sup>81</sup> is an experiment on a rat model of radiation-induced lung injury. By constructing an animal RILI acute phase model and detecting changes in serum cytokine levels after administration, no human clinical trial data were involved.
Shortened Absorption Time of Pulmonary Inflammation	Qingfei Detoxification Soup reduces the absorption time of lung inflammation by 33% (5.3 days vs 8.0 days)	Preclinical model (animal experiment)	The data is derived from the same animal experiment mentioned above, <sup>81</sup> and the absorption process of inflammatory lesions in the lungs of animals is observed through imaging (such as CT) and pathological sections, which belongs to the scope of preclinical research.
Reduction in the pulmonary fibrosis area	Huangqi Danshen medicine (3:1) blocks the TGF - $\beta$ /Smad3 pathway, reducing the area of pulmonary fibrosis by 62%	Preclinical model (animal experiment)	This data is from a mouse pulmonary fibrosis model study, <sup>82</sup> which quantifies the proportion of fibrotic areas in lung tissue using pathological detection methods such as Masson staining, and is the result of animal experiments.
Improvement in pulmonary function index (DLCO)	Huangqi Danshen medicine improves DLCO (diffusion capacity of carbon monoxide) by 12.7% in patients	Clinical trials (human studies)	The study <sup>82</sup> included a small sample clinical observation cohort (including 48 RILI chronic phase patients), and DLCO values were measured before and after administration using a pulmonary function detector, which belongs to human clinical trial data (phase II exploratory trial).
Reduction in the risk of adverse events	Traditional Chinese medicine compound reduces the total risk of RILI adverse events by 60% (RR=0.40) and the risk of hormone-related hyperglycemia by 68%	Clinical trials (summary analysis)	The data comes from meta-analysis, <sup>83</sup> which includes 8 published RILI clinical trials of traditional Chinese medicine treatment (526 patients in total), and summarizes and analyzes the safety indicators of human medication, which belongs to the summary results of clinical trial data.
Improvement in treatment adherence	Traditional Chinese Medicine Compound Increases Patient Treatment Compliance by 35%	Clinical trials (human studies)	This indicator is derived from the clinical trials included in the meta-analysis, <sup>83</sup> calculated by recording the patient's medication adherence rate (such as the number of times medication is taken on time/total number of times medication should be taken), based on the population statistics of human clinical trials.

precisely match the target area, which can increase the dose to the target area and at the same time reduce the dose to normal tissues.<sup>85</sup> Therefore, by precisely optimizing the radiotherapy protocol (eg, adjusting the angle of the irradiation field, optimizing the dose distribution, and adopting advanced techniques such as IMRT, VMAT, and SBRT), the irradiated dose and volume of normal lung tissues can be effectively reduced, which can significantly reduce the risk of RP. By optimizing the angle of the irradiation field and dose distribution, the irradiated range and radiation dose to the lung tissue can be effectively controlled, thus reducing the possibility of RILI. However, these techniques are not without risk. IMRT techniques, although effective in reducing the volume of the high-dose area, may result in a larger area of lung tissue receiving low-dose radiation, with a potential risk of inducing RILI. Therefore, when applying these techniques, patient-specific conditions need to be rigorously evaluated and radiotherapy regimens tailored to reduce RP risk.<sup>86</sup>

## Imaging Histology and Artificial Intelligence Assisted Therapy

Imaging histology combined with artificial intelligence technology provides an innovative solution for accurate diagnosis and treatment of RP. With the help of intelligent imageomics methods, some scholars extracted quantitative image features from patients' pre-treatment CT images and constructed a prediction model, which was able to efficiently assess the risk of RP.<sup>72–74</sup> Artificial intelligence (AI) technology can intelligently optimize radiotherapy parameters based on massive clinical case data and assist physicians in formulating personalized radiotherapy plans, thus improving treatment accuracy and effectively controlling RP risk.<sup>75</sup>

Beyond its established applications in risk stratification and radiotherapy planning, AI offers transformative potential in the context of NDDS-mediated therapy for RILI. By integrating radiomic features extracted from pre- and post-treatment imaging modalities—such as CT-derived texture patterns and density distributions indicative of inflammatory or fibrotic changes—with dosimetric parameters and patient-specific biomarkers (eg, serum levels of TGF- $\beta$  and IL-6), AI-driven models may enable accurate prediction of the spatial and temporal evolution of the pathological pulmonary microenvironment. These models can delineate critical variables, such as ROS gradients, pH fluctuations, and localized cytokine surges, within irradiated lung regions. Such predictive capabilities are instrumental in guiding the rational design and personalized deployment of NDDSs. For example, AI may inform the optimization of nanocarrier physico-chemical properties (eg, particle size, surface charge, ligand density) to enhance selective accumulation in regions identified as high-risk or pathologically active. This approach builds on methodological foundations established by Reuzé et al, who systematically demonstrated how CT or PET radiomic features, when combined with dose-volume parameters, can predict radiation-induced tissue damage—providing a framework for translating multi-modal data integration into AI-driven RILI modeling.<sup>87</sup> Additionally, AI could support the dynamic tuning of stimulus-responsive release thresholds in ROS- or pH-sensitive systems, based on predicted biomarker concentrations and environmental cues. Notably, Orhac et al detailed protocols for extracting high-order radiomic features (eg, texture, density distributions) and coupling them with serum biomarkers like TGF- $\beta$  and IL-6—key steps in training AI models to map pathological microenvironmental changes in irradiated lungs.<sup>88</sup> Furthermore, individualized dosing regimens—including timing, dosage, and administration route (eg, systemic versus inhalational)—could be tailored in real-time according to the projected course of RILI progression and early therapeutic response, thus enabling fully adaptive and precision-guided nanotherapeutic strategies. This real-time adaptability aligns with the AI decision frameworks reviewed by Danieli et al, which outline methods for personalized dose adjustment and optimal route selection (including inhalational versus systemic delivery)—directly translatable to NDDS temporal and spatial control.<sup>89</sup>

In the future, the combination of imaging/ AI technology and a nanomedicine delivery system to build a “diagnosis and treatment integration” platform is expected to achieve early and accurate prediction of the risk of RILI and guide the formulation and dynamic adjustment of personalized nanomedicine treatment plans. This integration (image/AI-guided personalized nanodiagnosis and treatment) is one of the essential directions for the future. This integration (imaging/AI-guided personalized nano-diagnosis and therapy) is one of the crucial future directions. Table 5 summarizes the current major therapeutic strategies for different stages of RILI and their evaluation.

**Table 5** RILI Staged Treatment Strategies and Evaluation

Staging/ Lesions	Main Therapeutic Objectives	Core Treatment Strategies	Representative Drugs/ Methods	Evaluation and Evidence	Ref
Acute phase (RP)	Controls inflammation and relieves symptoms	Glucocorticosteroid	Methylprednisolone, prednisone	Rapidly inhibits the release of inflammatory factors (TNF- $\alpha$ /IL-6) and relieves symptoms; Limitations: Limited efficacy against established RILF, risk of hyperglycemia/infection with long-term use	[77]
	Symptomatic support	Oxygen therapy/fever reduction/cough relief	Nasal tube oxygen, dextromethorphan	Improved quality of life, subject to strict indications (eg, SpO <sub>2</sub> <90%)	[90]
Chronic phase (RILF)	Slowing the Progression of Fibrosis	Antifibrotic drugs	Pirfenidone, Nidanib	Inhibition of the TGF- $\beta$ /Smad3 pathway reduces collagen deposition; Limitations: only delayed decline in lung function (eg, $\downarrow$ 50% annual decline in FVC); Incidence of gastrointestinal side effects >20%	[9,10,78]
		Combine traditional Chinese and Western medicine	Astragalus-Danshen medicinal pair, Clearing the Lungs and Removing Toxins Soup	Reduction in serum IL-6/TNF- $\alpha$ levels (~45%), fibrosis area (~62%); Reduction in overall adverse events (~60%)	[81–83]
Cross- cutting/ prevention	Reducing the risk of RILI	Optimization of radiotherapy techniques	IMRT, VMAT, SBRT	Reduced lung V20 (irradiated >20 Gy volume), but may increase low-dose exposure volume	[85,86]
		Antioxidant protection	HfO <sub>2</sub> NPs, SP@ASXnano	HfO <sub>2</sub> NPs scavenge ROS $\uparrow$ , radiation survival increased to 78%; SP@ASXnano boosts intestinal drug AUC 40-fold	[91,92]
Exploratory Directions	Targeted Intervention Core Mechanisms	Nano drug delivery systems	HA NPs, nucleic acid-carrying exosomes	HA NPs modulate TGF- $\beta$ 1/MMP-9 signaling; Exosomal delivery of miR-21 inhibitor suppresses TGF- $\beta$ 1/Smad3 signaling	[93]
		Cytokine modulator	TGF- $\beta$ inhibitor, anti-PDGF antibody	Preclinical studies: Anti-TGF- $\beta$ antibody ameliorates fibrosis in animal models	[50]

## Advances in NDDSs for RILI

RILI, encompassing early-stage RP and late-stage RILF, remains a common and serious complication following thoracic radiotherapy. The complex pathophysiological processes underlying RILI pose significant clinical challenges, particularly given the limited efficacy and substantial side effects—such as hyperglycemia and immunosuppression—associated with conventional high-dose corticosteroid therapy. NDDSs offer a promising alternative due to their unique advantages, including multifunctional loading capacity, enhanced targeting specificity, improved bioavailability, reduced systemic toxicity, and controllable or stimuli-responsive drug release profiles.<sup>94,95</sup> As illustrated in Figure 3, current research on NDDSs for RILI treatment primarily centers around two strategic directions. The first involves the direct application of nanomaterials with intrinsic antioxidative, anti-inflammatory, or antifibrotic properties (eg, HfO<sub>2</sub> nanoparticles, CeO<sub>2</sub> nanoparticles, and

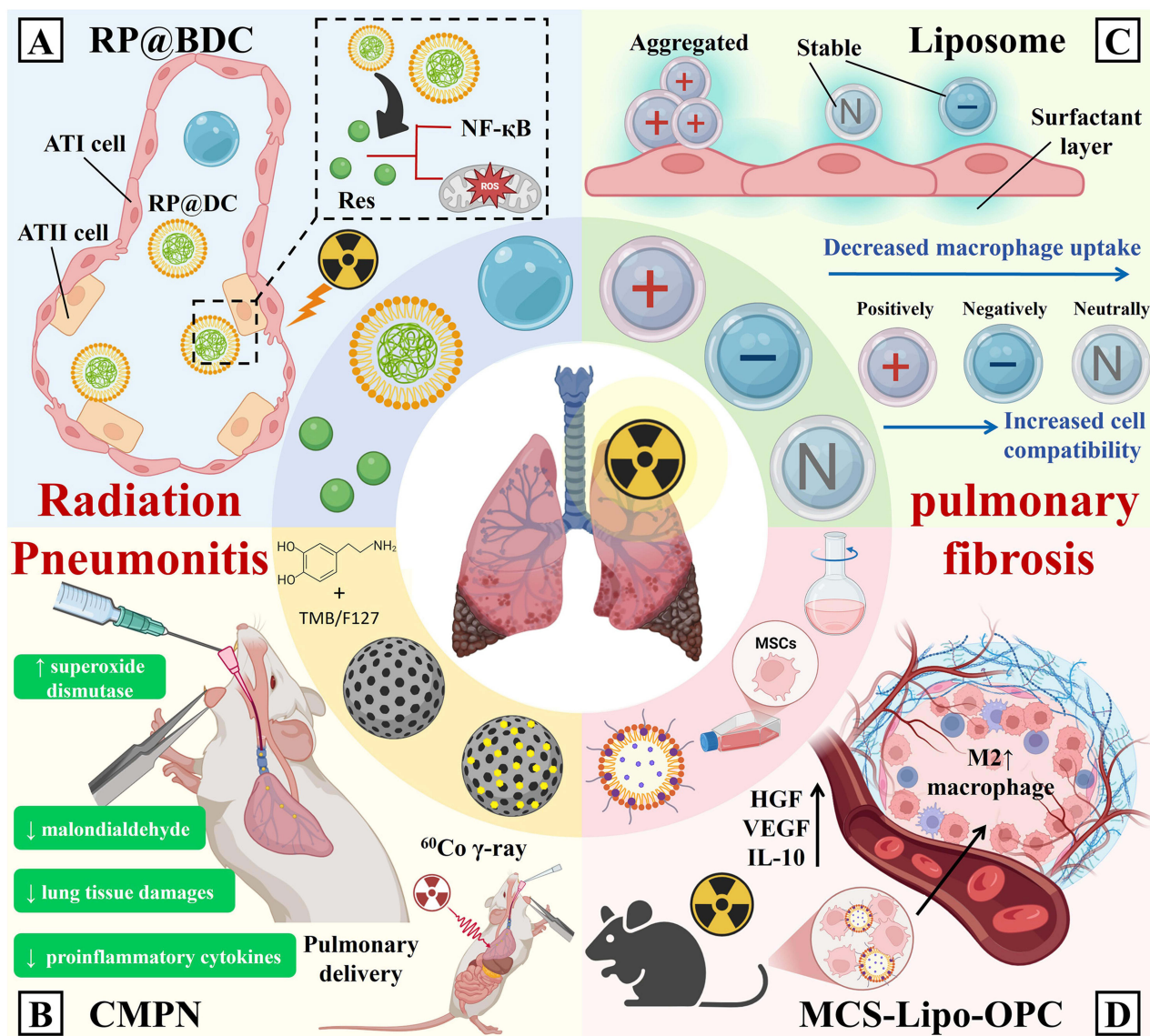


**Figure 3 (A–D)** Schematic illustration of nanomedicine delivery systems for RILI treatment. This figure depicts key nanomedicine-based therapeutic strategies for radiation-induced lung injury (RILI), including inhibition of inflammation, alleviation of oxidative stress, and attenuation of fibrosis, with a focus on the underlying biological mechanisms. Representative systems shown include: inhalable multilevel responsive microspheres (RP@BDC), which utilize pH sensitivity (triggered by the acidic microenvironment of irradiated lungs) for co-delivery of anti-inflammatory resveratrol and anti-fibrotic siPAI-1 to target both inflammatory and fibrotic pathways; curcumin-loaded mesoporous polydopamine nanoparticles (CMPN), which achieve synergistic ROS scavenging through curcumin and polydopamine, with high drug-loading capacity and accelerated release for enhanced pulmonary deposition; surface charge-regulated inhaled liposomes, where charge modulation (neutral/positive) reduces macrophage uptake and improves cellular compatibility to boost local drug concentration; and liposome-anchored mesenchymal stem cells (MSC-Lipo-OPC), in which MSCs target inflamed lung tissues and anchored liposomes deliver antioxidants (OPC) to scavenge ROS, regulating M2 macrophage polarization and promoting tissue repair via secretion of IL-10 and VEGF.

hyaluronic acid-based nanoparticles) to modulate pathological processes. The second focuses on the development of innovative nanocarrier systems capable of site-specific delivery and microenvironment-responsive release of therapeutic agents, including anti-inflammatory/antioxidant compounds, antifibrotic drugs, and nucleic acid therapeutics, targeting injured pulmonary tissue. These systems often exploit pathophysiological cues such as elevated ROS or aberrant pH to trigger drug release, thereby enhancing therapeutic efficacy while minimizing off-target effects. The rapid progress in NDDS development holds considerable promise for designing safer and more effective therapeutic strategies for RILI, offering new avenues for clinical translation in the management of radiation-associated pulmonary complications.<sup>95,96</sup>

## Polymer-Based Nanocarriers

Polymer-based nanocarriers, derived from either natural or synthetic polymers, offer a versatile platform for the prevention and treatment of RILI. These systems exert therapeutic effects either through the encapsulation and controlled delivery of pharmacological agents or via the intrinsic physicochemical and biological properties of the polymers themselves. Their principal advantages include excellent biocompatibility, biodegradability, and the potential for controlled and sustained drug release. By tailoring parameters such as particle morphology, size, and surface functionalization, these nanocarriers can achieve favorable biodistribution profiles and targeted pulmonary delivery, thereby enhancing drug stability and therapeutic efficacy. Recent progress in this field is summarized below, categorized by carrier type.

## Synthetic Polymer-Based Carriers

### PLGA Microspheres for Passive Targeting and Sustained Release

Poly(lactic-co-glycolic acid) (PLGA), an FDA-approved biodegradable polymer, has demonstrated significant promise in RILI management, particularly due to its passive lung-targeting properties and controlled release kinetics. Using membrane emulsification, PLGA microspheres with an average diameter of 17  $\mu\text{m}$  were prepared, achieving a high drug loading efficiency (24.97%) for rosmarinic acid (RA). These microspheres effectively inhibited M2 macrophage polarization, as evidenced by downregulation of CD206, IL-10, and Arg-1, and significantly suppressed profibrotic mediator TGF- $\beta$ 1 (by 52.4%) and epithelial–mesenchymal transition (EMT) marker  $\alpha$ -SMA (by 28.3%). The large particle size facilitated mechanical entrapment within pulmonary capillaries, enabling prolonged lung retention (>1 week) and extended in vitro release over 7 days. In a murine model of lung fibrosis induced by 15 Gy thoracic irradiation, treatment with RA-loaded PLGA microspheres improved inspiratory capacity by 57.8% and reduced fibrotic area by 40%.<sup>97,98</sup>

### PLGA Nanoparticles for Gene Pathway Modulation

PLGA nanoparticles encapsulating melatonin (MET/PLGANPs), prepared via nanoprecipitation and solvent evaporation, exhibited a mean diameter of ~98.7 nm and an encapsulation efficiency of 68.1%. Following intratracheal administration, the nanoparticles achieved localized pulmonary deposition with a retention time exceeding 4 h. Mechanistically, MET/PLGANPs attenuated alveolar epithelial cell apoptosis by modulating the miR-21/TGF- $\beta$ 1/Smad3 signaling axis, resulting in a 35% reduction in caspase-3 activity and offering a promising strategy for mitigating post-radiation inflammation and fibrotic progression.<sup>99</sup>

## Natural Polymer-Based Carriers

Natural biopolymers such as chitosan, alginate, and hyaluronic acid (HA) are garnering significant interest due to their intrinsic biocompatibility, biodegradability, and therapeutic activity, either inherently or upon drug loading.

### Injectable Chitosan-Based Hydrogel for Antioxidant and Antifibrotic Therapy

Schiff base crosslinking of chitosan, astragalus gum, and cellulose nanocrystals developed an injectable and self-healing composite hydrogel. Administered intraperitoneally at 25 mg/kg, the hydrogel effectively localized to lung tissues. In irradiated rats, treatment significantly enhanced pulmonary antioxidant enzyme activity, increasing superoxide dismutase (SOD) to 52 IU/mL and glutathione peroxidase (GPx) to 37 IU/mL, while reducing malondialdehyde (MDA) to 10  $\mu\text{M}$ —

approaching normal levels. In a 15 Gy radiation model over 50 days, the hydrogel reduced alveolar wall thickness by 60% and collagen deposition by 50%, indicating substantial mitigation of radiation-induced lung pathology.<sup>100</sup>

## HA-Based Nanoparticles with Intrinsic Anti-Inflammatory Activity

Hyaluronic acid (HA), a high-molecular-weight glycosaminoglycan, exhibits innate anti-inflammatory and tissue repair properties. HA nanoparticles (HA NPs), formed via crosslinking, modulated key fibrotic pathways including TGF- $\beta$ 1 and matrix metalloproteinases (MMP-2/MMP-9), while maintaining tissue redox homeostasis. HA NPs significantly attenuated lung inflammation and fibrosis post-radiation. Notably, nanoparticle size played a pivotal role in immunomodulation and tissue regeneration, offering a promising, biocompatible option for RILI intervention.<sup>93</sup>

Lierova et al investigated the therapeutic potential and underlying mechanisms of hydroxyapatite nanoparticles (HAp NPs) in mitigating RIPI.<sup>93</sup> Two formulations of biocompatible HAp NPs, with mean diameters of 86.58 nm and 123.6 nm, were synthesized via single and dual crosslinking strategies, respectively. Physicochemical characterization demonstrated their sustained stability following exposure to 17 Gy  $\gamma$ -irradiation and negligible cytotoxicity toward the murine macrophage cell line J774.2. In vivo, HAp NPs were administered via intratracheal instillation to C57Bl/6 mice 30 minutes before thoracic irradiation with a single 17 Gy dose. At post-irradiation time points corresponding to key stages of RIPI—days 113, 155, and 190—molecular, cellular, and histopathological parameters were assessed in lung tissue and peripheral blood. The results revealed that HAp NP treatment significantly modulated the expression of cytokines within lung tissue, particularly those implicated in profibrotic signaling pathways. Notably, levels of transforming growth factor- $\beta$  (TGF- $\beta$ ) and matrix metalloproteinase-2 (MMP-2) were reduced, and the balance between MMP-2 and its precursor MMP-9 was restored. Peripheral leukocyte profiles were also influenced by HAp NP administration. On day 113 (corresponding to the inflammatory pneumonitis phase), mice treated with 86.58 nm HAp NPs exhibited increased total leukocyte counts, whereas the 123.6 nm HAp NPs group showed a marked rise in neutrophil counts. By day 190 (fibrotic phase), the irradiated group displayed elevated lymphocyte levels, whereas the HAp NP-treated groups showed values comparable to those of non-irradiated controls. These findings suggest that HAp NPs confer protection against RIPI by modulating cytokine-mediated signaling, immune cell infiltration, and tissue remodeling processes. This study provides promising evidence supporting the use of HAp NPs as a nanotherapeutic strategy for preventing and treating radiation-induced pulmonary fibrosis.

## Bioengineered Nanoreactors (SOD@ARA290-HBc)

Liu et al developed a bioengineered nanoreactor (SOD@ARA290-HBc) and systematically evaluated its multifaceted therapeutic potential in mitigating RILI.<sup>101</sup> This nanoplatform was constructed using hepatitis B core (HBc) virus-like particles (VLPs) as a nanocarrier scaffold. Through genetic engineering, the erythropoietin-derived peptide ARA290—lacking erythropoietic activity but retaining tissue-protective properties—was integrated into the structural framework of HBc. Subsequently, superoxide dismutase (SOD) enzymes were encapsulated within the nanoreactor via disassembly/reassembly processes, resulting in efficient loading. Characterization studies revealed that SOD@ARA290-HBc nanoparticles are monodisperse, spherical structures with an average diameter of  $\sim$ 35 nm, capable of encapsulating approximately 63 SOD molecules per particle. This formulation markedly enhanced the pulmonary stability and enzymatic retention of SOD, while simultaneously prolonging the half-life of ARA290 and reducing its immunogenicity. In a murine model of RILI, intratracheal administration of SOD@ARA290-HBc led to significant amelioration of both acute radiation pneumonitis and subsequent pulmonary fibrosis. Mechanistic investigations demonstrated that the nanoreactor exerts its protective effects through multiple pathways: (1) preserving alveolar epithelial cell integrity by attenuating radiation-induced apoptosis and ferroptosis; (2) suppressing oxidative stress by decreasing malondialdehyde (MDA) levels and restoring SOD and glutathione peroxidase (GSH-Px) activity; (3) mitigating inflammatory responses by reducing proinflammatory cytokines (TNF- $\alpha$ , IL-1 $\beta$ ) and neutrophil infiltration; and (4) modulating immune responses via macrophage polarization toward the anti-inflammatory M2 phenotype. Collectively, these findings underscore the potential of SOD@ARA290-HBc as a multifunctional nanotherapeutic agent for the effective prevention and treatment of RILI, offering a promising strategy for clinical translation.

## Polymer–Microalgae Hybrid Systems

A novel oral delivery platform integrating *Spirulina* (SP) microalgae with astaxanthin-loaded nanoparticles (ASXnano) was developed, forming the composite SP@ASXnano system.<sup>91</sup> Electrostatic interactions between negatively charged SP and cationic chitosan/PLGA-coated ASXnano ( $\zeta$ -potential +67.3 mV) yielded hybrid particles with an average size of ~203 nm. SP's helical structure and microscale dimensions enabled prolonged intestinal retention (>12 h), supporting gradual release of ASXnano. Astaxanthin scavenged radiation-induced ROS, while SP contributed to endogenous antioxidant defense by enhancing SOD and GPx activity. Importantly, SP@ASXnano modulated gut microbiota composition, increasing beneficial genera such as *Akkermansia* and *Lactobacillus*, and elevated short-chain fatty acid (SCFA) levels—particularly butyrate, which increased 2.5-fold. This modulation of the gut–lung axis effectively suppressed pulmonary inflammation. In a 10 Gy whole-body irradiated mouse model, SP@ASXnano extended median survival from 11.5 to 29 days, reduced intestinal ROS by 45%, and elevated peripheral leukocyte and platelet counts by 30%, suggesting restoration of hematopoietic function.

## Inorganic Nanocarriers

Inorganic nanoparticles, particularly metal oxides such as hafnium oxide (HfO<sub>2</sub>) and cerium oxide (CeO<sub>2</sub>), have garnered considerable attention as potential therapeutic agents for RILI, owing to their intrinsic multi-enzyme mimetic activities (eg, SOD, CAT, GPx), their ability to scavenge ROS, and their organ-targeting potential.

### Hafnium Oxide Nanoparticles (HfO<sub>2</sub> NPs)

HfO<sub>2</sub> nanoparticles exhibit size-dependent organotropism, which can be tailored via  $\alpha$ -lactalbumin-mediated synthesis. Particles of approximately 122.9 nm preferentially accumulate in pulmonary tissue, whereas particles of 30 nm and 2.4 nm predominantly localize in the liver and kidneys, respectively. This size-selective biodistribution provides a basis for the rational design of lung-targeted radioprotective strategies. In addition to targeting capabilities, HfO<sub>2</sub> NPs serve as effective CT imaging contrast agents due to the high K-edge energy (65.4 keV) of hafnium.

Functionally, HfO<sub>2</sub> NPs display potent ROS scavenging properties, mimicking SOD, CAT, and GPx activities with a reported ROS clearance efficiency 1.5 times higher than that of conventional CeO<sub>2</sub> NPs.<sup>92</sup> Mechanistically, they modulate critical signaling pathways such as FoxO, Hippo, and TNF, thereby attenuating radiation-induced oxidative stress and inflammation. Experimental data indicate that HfO<sub>2</sub> NPs reduce  $\gamma$ -H2AX foci formation by 60% and suppress proinflammatory cytokines IL-6 and TNF- $\alpha$  by 50%. In vivo, lung-targeted HfO<sub>2</sub> NPs improved survival to 78% in a rabbit model subjected to 20 Gy total-body irradiation, accompanied by a two-fold increase in pulmonary SOD activity and a 40% reduction in malondialdehyde (MDA) levels, confirming their significant radioprotective efficacy.<sup>92</sup>

### Cerium Oxide Nanoparticles (CeO<sub>2</sub> NPs)

CeO<sub>2</sub> NPs possess inherent redox cycling between Ce<sup>3+</sup> and Ce<sup>4+</sup> states, enabling sustained ROS scavenging. Surface PEGylation enhances their colloidal stability and biocompatibility, yielding core nanoparticles with a diameter of approximately 5 nm. These NPs can serve as delivery vehicles for therapeutic microRNAs such as miR-146a, constructing a multifunctional platform for RILI intervention.

Upon inhalation, the CeO<sub>2</sub>-miR-146a nanocomposite exhibits ~35% alveolar deposition and is designed for ROS-responsive release, ensuring site-specific miRNA delivery in the oxidative microenvironment of injured lung tissue.<sup>102</sup> The therapeutic effect is exerted via dual mechanisms: (1) CeO<sub>2</sub>-mediated continuous ROS neutralization, and (2) miR-146a-mediated suppression of TLR4/NF- $\kappa$ B signaling, which significantly reduces inflammatory cytokines IL-6 and IL-1 $\beta$ —in a murine model of acute lung injury induced by 15 Gy irradiation, treatment with this system for seven days resulted in a 55% reduction in the area of inflamed tissue and a 45% decrease in neutrophil infiltration.

Furthermore, advanced composite nanoplatforms such as NPs Ce(phen)Pirf<sub>3</sub> (cerium-1,10-phenanthroline-pirfenidone nanocomplexes) have demonstrated improved lung function and alleviated radiation-induced pathological changes in lung tissues following irradiation.<sup>103</sup> These nanocomplexes reduce fibrosis-related collagen deposition and regulate epithelial–mesenchymal transition (EMT)-associated markers, including  $\alpha$ -SMA and TGF- $\beta$ 1 (down-

regulating their expression) while up-regulating E-cadherin and down-regulating N-cadherin, thereby inhibiting the progression of RIPP.

## Stimuli-Responsive Nanocarriers

RILI is characterized by a distinct inflammatory microenvironment, where elevated levels of ROS and localized acidification—attributable to immune cell activation and metabolic alterations—are commonly observed.<sup>104</sup> Stimuli-responsive nanocarriers are designed to respond to such pathological cues (eg, high ROS levels and low pH) by triggering site-specific drug release, thereby enhancing spatial and temporal precision of therapy, minimizing off-target distribution, and reducing systemic toxicity.

## ROS-Responsive Systems

Wang et al developed chitosan-based microspheres (CS-PBA-Cro, Figure 4) with a mean diameter of approximately 10  $\mu\text{m}$  for the pulmonary delivery of crocin-I (Cro), a natural antioxidant compound.<sup>105</sup> The formulation was modified with phenylboronic acid (PBA), which forms boronate ester bonds with vicinal diols in Cro, rendering the system sensitive to ROS. In the presence of elevated  $\text{H}_2\text{O}_2$  (>100  $\mu\text{M}$ ), these boronate linkages undergo rapid cleavage, leading to controlled and stimulus-responsive drug release. The microspheres exhibited prolonged pulmonary retention (>48 hours) and passive lung targeting due to their size. Therapeutic evaluation revealed that, seven days post 20 Gy irradiation, CS-PBA-Cro

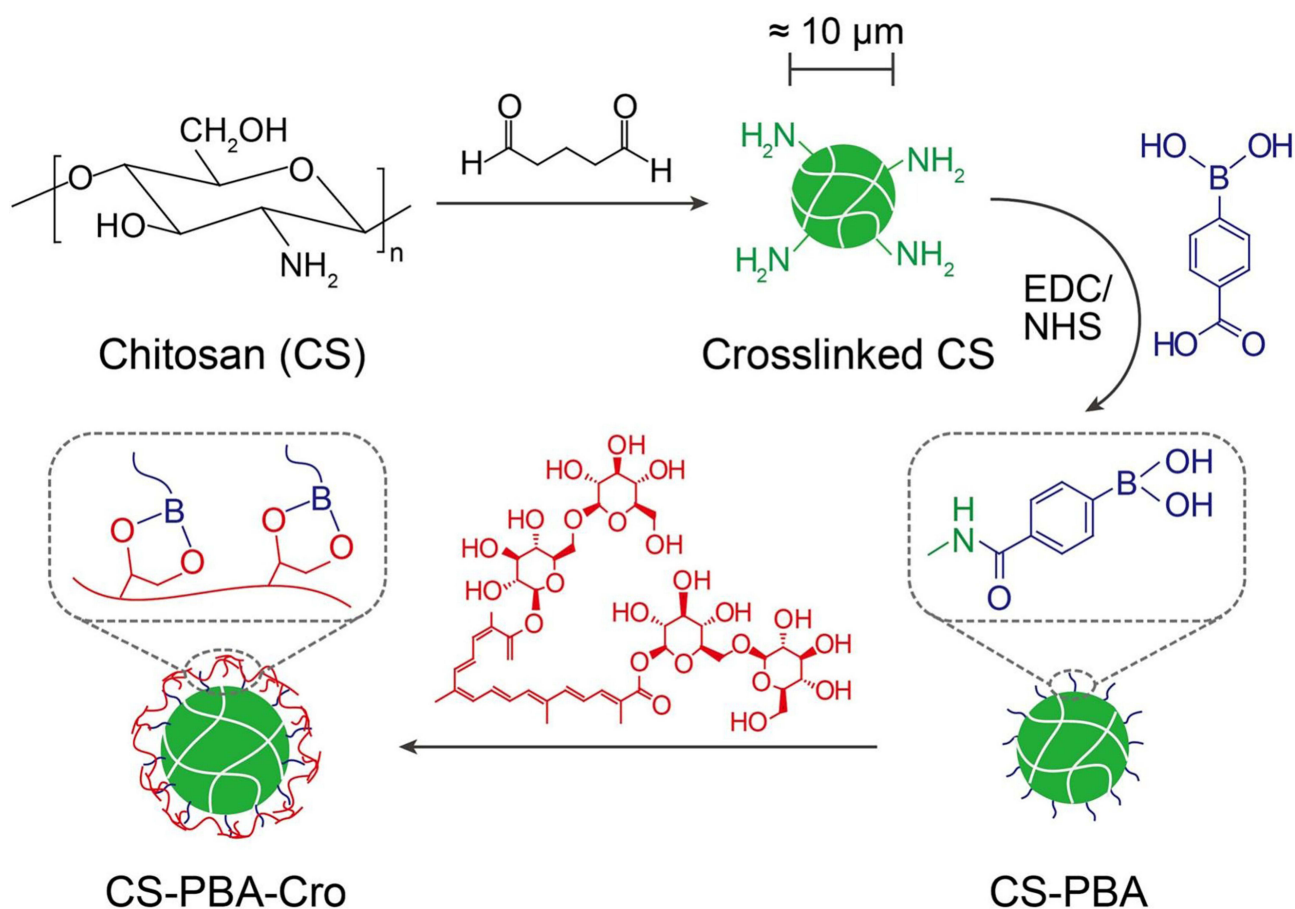


**Figure 4** Schematic diagram of crocin-loaded ROS-responsive chitosan microspheres (CS-PBA-Cro) for passive lung targeting. The microspheres ( $\approx 10 \mu\text{m}$ ) are modified with phenylboronic acid (PBA), which forms boronate ester bonds with crocin (Cro) to stabilize the structure. In the high-ROS microenvironment of irradiated lungs ( $\text{H}_2\text{O}_2 > 100 \mu\text{M}$ ), these bonds cleave rapidly, triggering controlled release of Cro (a natural antioxidant). This design enables prolonged pulmonary retention (>48 h), passive targeting via mechanical entrapment in pulmonary capillaries, and site-specific drug release to attenuate radiation-induced inflammation and oxidative damage. (Reproduced with permission from reference.<sup>105</sup>) Used from Wang L, Liu C, Lu W, et al. ROS-sensitive Crocin-loaded chitosan microspheres for lung targeting and attenuation of radiation-induced lung injury. *Carbohydrate polymers*. 2023; 307:120628. Permission conveyed through Copyright Clearance Centre, Inc.

significantly attenuated inflammation, enhanced antioxidant enzyme activity, and decreased malondialdehyde (MDA) levels by 40%, along with a 25% reduction in alveolar wall thickness, demonstrating pronounced radioprotective efficacy.

## pH-Responsive and Multi-Stimuli Delivery Systems

To address the acidic milieu of RILI lesions, Wang et al further developed an innovative, inhalable, multi-stimuli-responsive microsphere system (RP@BDC), composed of  $\beta$ -cyclodextrin-based nanoparticles co-loaded with resveratrol (Res; an anti-inflammatory NF- $\kappa$ B inhibitor) and siRNA targeting plasminogen activator inhibitor-1 (siPAI-1; an anti-fibrotic agent).<sup>106</sup> The nanoparticles were encapsulated within chitosan and modified with dipalmitoylphosphatidylcholine (DPPC) to facilitate mucus penetration and alveolar epithelial adhesion. Calcium carbonate mineralization was employed to fabricate a protective shell, yielding microspheres with a diameter of 2–3  $\mu$ m, suitable for inhalation and deep lung deposition. Critically, the  $\text{CaCO}_3$  layer conferred pH sensitivity—rapidly dissolving under acidic conditions (pH  $\sim$ 6.2, typical of irradiated lung tissues) within 30 minutes to release the inner drug-loaded core (RP@DC), while maintaining structural stability under physiological pH (7.4). The synthesis process, delivery route, and pharmacodynamic mechanism of this multifunctional system are illustrated in Figure 5. This environment-specific release strategy enables precise spatiotemporal delivery, concurrently targeting inflammatory and fibrotic pathways while minimizing off-target effects.<sup>106</sup>

## Biological Signal-Responsive Targeted Systems

Guan et al developed a bioresponsive and lung endothelium-targeted fusion system, LET-bFGF, designed to mitigate RILI.<sup>107</sup> This system comprises a synthetic targeting peptide (LET; sequence: CGSPGWVRC) conjugated to basic fibroblast growth factor (bFGF), forming a fusion protein that selectively accumulates in injured pulmonary tissue. The

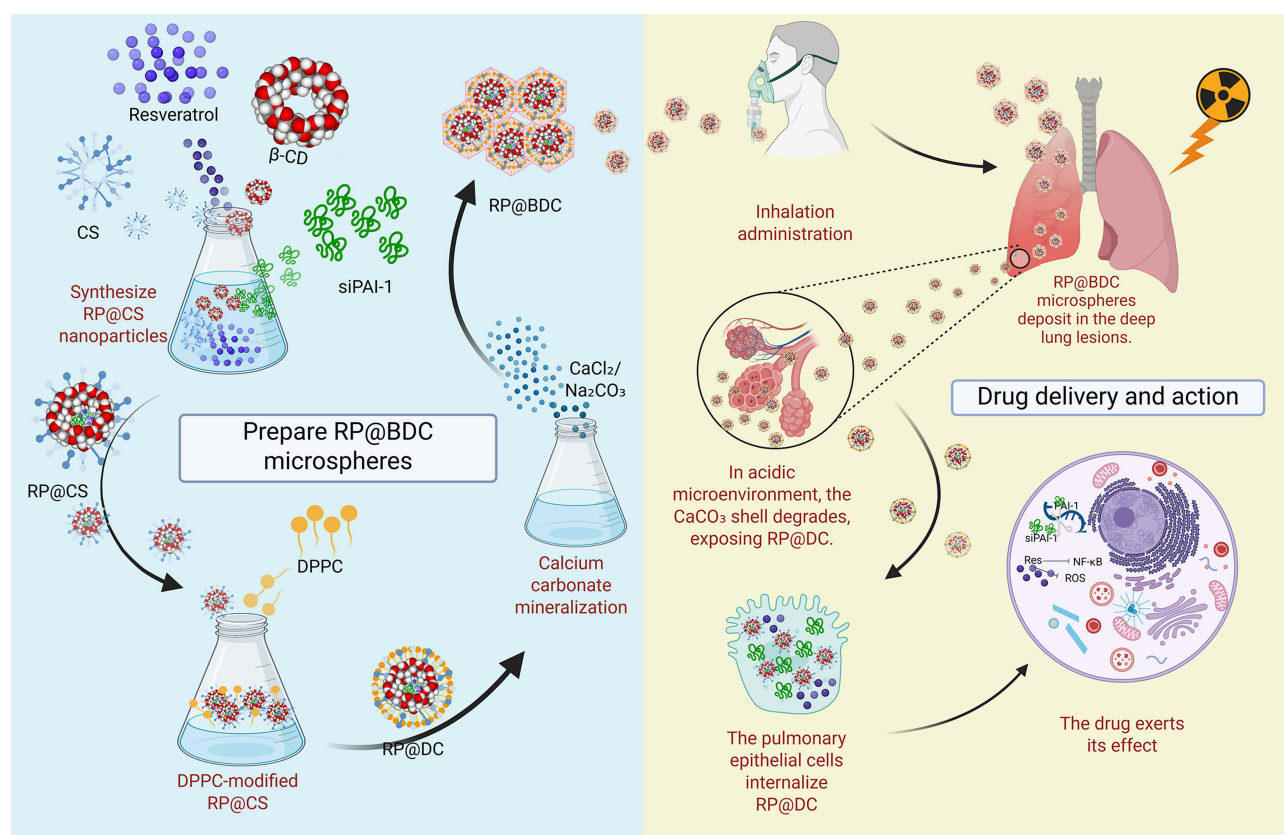


**Figure 5** Schematic illustration of the RP@BDC microsphere system. The system is prepared through the co-assembly of resveratrol (Res), siPAI-1,  $\beta$ -cyclodextrin ( $\beta$ -CD), and chitosan (CS), followed by calcium carbonate mineralization and DPPC modification to form inhalable RP@BDC microspheres. Upon pulmonary delivery, the  $\text{CaCO}_3$  shell degrades in the acidic lung microenvironment, releasing RP@DC, which is internalized by epithelial cells to exert anti-inflammatory and anti-fibrotic effects. Image created with BioRender.com, with permission.

LET peptide specifically recognizes aberrant molecular signals presented on the surface of irradiated pulmonary endothelial cells—such as upregulated receptors or chemokine gradients—enabling precise enrichment of bFGF at sites of tissue damage. Quantitative biodistribution analysis revealed that LET-bFGF achieves 1.5–2-fold greater accumulation in irradiated lung tissue compared to unmodified bFGF, with minimal off-target distribution in healthy organs, highlighting its dynamic responsiveness to pathological microenvironments. A 15-amino acid flexible linker was employed to connect LET and bFGF, maintaining the structural integrity and biological activity of bFGF while ensuring efficient conjugation. In a rat model subjected to 15 Gy thoracic irradiation, intravenous administration of LET-bFGF (25 nmol/kg) resulted in pronounced therapeutic effects. Four hours post-irradiation, LET-bFGF reduced pulmonary endothelial cell apoptosis by approximately 40% relative to native bFGF. At two months post-irradiation, treated animals exhibited significant improvements in histopathological parameters, including a 40% reduction in vascular wall thickening, a 50% decrease in CD45<sup>+</sup> inflammatory cell infiltration, and attenuation of pulmonary density increases. Moreover, LET-bFGF mitigated structural disorganization and fibrotic remodeling within lung tissues. These findings suggest that LET-bFGF represents a promising targeted therapeutic strategy for RILI and exemplifies the potential of bioresponsive targeting systems for precision intervention in inflammation- and injury-associated diseases.

## Nucleic Acid Delivery-Based Nanoplatfoms

In fibrotic diseases such as RILF, aberrant activation of key signaling pathways—particularly the TGF- $\beta$ /Smad axis—serves as a central driver of disease progression. Targeted modulation of these pathogenic gene expressions through advanced genetic technologies, including CRISPR/Cas9-mediated genome editing and RNA interference via miRNA or siRNA, represents a cutting-edge strategy for interrupting dysregulated signal transduction and achieving precision therapy. Nucleic acid-based interventions have shown substantial promise in preventing and treating RILF, especially for individuals requiring long-term pulmonary protection, such as patients undergoing thoracic radiotherapy or those exposed to nuclear incidents.<sup>108</sup>

### CRISPR/Cas9-Based Genome Editing

The CRISPR/Cas9 system provides a powerful gene-editing tool for selectively silencing pivotal fibrogenic mediators in RILI. Zhen et al developed an adenovirus-delivered CRISPR/Cas9 system (Ad-CRISPR-TGF- $\beta$ 1) specifically targeting the TGF- $\beta$ 1 gene.<sup>109</sup> Upon intravenous administration, the system induced site-specific double-stranded DNA breaks within the TGF $\beta$ 1 locus via Cas9 endonuclease, triggering error-prone non-homologous end joining (NHEJ) repair that resulted in loss-of-function mutations. This gene disruption resulted in significant downregulation of TGF- $\beta$ 1 expression, a key pro-inflammatory and pro-fibrotic cytokine, thereby reducing inflammatory cytokine secretion and suppressing downstream fibrogenic signaling pathways. Notably, experimental results demonstrated a marked inhibition of TGF- $\beta$ 1 downstream effectors, such as connective tissue growth factor (CTGF) and alpha-smooth muscle actin ( $\alpha$ -SMA), at both the mRNA and protein levels. Interestingly, suppression of TGF- $\beta$ 1 also influenced the expression of other fibrogenic axes, including the SK1/S1P receptor 1 (S1PR1) pathway. Collectively, Ad-CRISPR-TGF- $\beta$ 1 therapy significantly mitigated pulmonary fibrosis in irradiated lungs, highlighting the translational potential of gene editing for RILF intervention.<sup>109</sup>

Despite these advantages, CRISPR/Cas9-based therapies present notable challenges, including the risk of off-target genome editing, unpredictable immune responses, and persistent ethical considerations. These issues warrant rigorous investigation and careful mitigation strategies before such approaches can be safely advanced toward clinical translation.

### miRNA Delivery Systems

MicroRNAs (miRNAs) regulate a broad spectrum of gene networks involved in inflammation and fibrosis, making them attractive therapeutic candidates for RILI. Stephen et al investigated the use of cerium oxide nanoparticles (CNPs) as carriers for therapeutic miRNAs such as miR-146a. CNPs possess an intrinsic redox cycling capability (Ce<sup>3+</sup>/Ce<sup>4+</sup>), enabling ROS scavenging, along with anti-inflammatory properties via the inhibition of TGF- $\beta$  and NF- $\kappa$ B pathways. As nanocarriers, CNPs enhance miRNA stability, facilitate cellular uptake by neutralizing negative surface charge, and overcome barriers to in vivo delivery. The researchers synthesized a CNP-miR-146a complex and administered it via intratracheal instillation. In vivo studies demonstrated enhanced miR-146a accumulation in lung tissues with minimal systemic distribution, indicating efficient pulmonary targeting. In a bleomycin-induced acute lung injury (ALI) model,

CNP-miR-146a treatment attenuated inflammatory cell infiltration, suppressed oxidative stress and inflammatory responses, and improved lung biomechanics. Mechanistically, the anti-inflammatory effects were primarily attributed to miR-146a-mediated inhibition of the TLR4/NF- $\kappa$ B signaling pathway. Although validated in an ALI model, this dual-function nanoplatfrom—combining nucleic acid delivery and bioactive inorganic nanoparticles—offers a promising therapeutic paradigm for managing RILI.<sup>102</sup>

## Inhalable Nanomedicines

Inhalable nanomedicines can traverse physiological barriers, engage in molecular-level interactions, and exert both local and systemic effects. Their therapeutic efficacy is closely associated with particle size, surface properties, and exposure dose. Leveraging the inherent advantages of nanoparticle-based delivery and the anatomical and physiological characteristics of the respiratory tract, inhalable nanosystems offer a closed-loop therapeutic approach characterized by targeted pulmonary deposition, high local drug concentration, and minimal systemic exposure. This strategy holds great promise for achieving both precision and safety in the treatment of respiratory diseases.

## Nanogels and Nanosuspensions

Chen et al developed an inhalable quercetin-alginate nanogel (QU-Nanogel), which is composed of quercetin and sodium alginate, using emulsion polymerisation. This “material-drug” nanocarrier system fixes quercetin through Ca<sup>2+</sup> cross-linking and hydrogen bonding to form a “co-construct” water-soluble system that significantly enhances quercetin’s solubility and bioavailability. This facilitates the release of its intrinsic antioxidant and anti-inflammatory properties. The nanogel has a uniform particle size (hydrodynamic average size of 61.87 nm, which is below 100 nm) and excellent biocompatibility. It exhibits superior cytoprotective effects, such as reducing paraquat-induced A549-GFP cell death, and has more potent antioxidant activity than free quercetin, as demonstrated by its greater DPPH scavenging and ferric reducing capacity. In a paraquat-induced rat model of ALI, ultrasonic nebulisation of the nanogel produced favourable therapeutic results, such as improving lung morphology (via microCT and histopathology), reducing inflammation (by downregulating TNF- $\alpha$ , IL-6, and IL-1 $\beta$  mRNA and protein), decreasing oxidative stress (by lowering MDA and increasing CAT), and preventing subsequent pulmonary fibrosis. These findings suggest that QU-Nanogel may serve as a promising inhalable platform for ALI treatment.<sup>110</sup>

Nanosuspensions—drug dispersion systems composed of nanosized drug particles suspended in a solvent—address the solubility challenges of hydrophobic drugs, which often exhibit high affinity for hydrophobic receptor pockets.<sup>111</sup> Su et al<sup>112</sup> prepared an inhalable nanosuspension of tetrandrine-hydroxypropyl- $\beta$ -cyclodextrin inclusion complexes (mean diameter: 640.3  $\pm$  49.2 nm) via high-pressure homogenization for bleomycin-induced pulmonary fibrosis. The formulation exhibited enhanced uptake kinetics, improved solubilization, and notable anti-inflammatory and antifibrotic effects, including suppression of hydroxyproline accumulation, regulation of fibrosis-associated protein expression, and a significant increase in survival rates in animal models.

Jackson et al developed a nanosuspension formulation of genistein, termed BIO 300, as a nanotherapeutic strategy for the prevention and mitigation of RILI.<sup>113</sup> Utilizing a proprietary wet-milling nanotechnology platform, hydrophobic genistein was processed into a nanosuspension with a mean particle size of less than 0.2  $\mu$ m, thereby significantly enhancing its aqueous solubility and systemic bioavailability. In pharmacokinetic studies, BIO 300 demonstrated approximately a two-fold increase in systemic exposure in mice and a five-fold increase in canines compared to non-nanosized formulations. The nanoformulation further promoted localized accumulation within pulmonary tissues, leveraging particle size-mediated passive targeting effects. Therapeutic efficacy was evaluated in C57L/J mouse models subjected to whole-thorax lung irradiation (WTLI) at doses of 11.0 Gy or 12.5 Gy. Oral administration of BIO 300 at 400 mg/kg, initiated 24 hours post-irradiation and continued for 4–6 weeks, significantly improved radiation outcomes. Notably, treated animals exhibited a 14–26.6% increase in 180-day survival rates relative to untreated controls, reduced respiratory frequency, and improved pulmonary function, as evidenced by decreased enhanced pause (Penh) values. Histopathological assessment revealed a ~40% reduction in fibrotic scarring, along with attenuation of pulmonary edema, congestion, and airway loss. Mechanistic investigations suggest that BIO 300 mediates its protective effects through suppression of oxidative stress and downregulation of key inflammatory (TNF- $\alpha$ , IL-1 $\beta$ ) and profibrotic (TGF- $\beta$ )

cytokines. These findings support BIO 300 as a practical and efficacious nanosuspension-based intervention for RILI and underscore the broader utility of nanonization strategies for enhancing the therapeutic performance of poorly water-soluble compounds in pulmonary injury and related pathologies.

## Dry Powder Inhalers (DPIs)

RP, a severe complication of thoracic radiotherapy in cancer patients, is often associated with respiratory distress and poor clinical outcomes. To address this challenge, Chen et al developed a dry powder inhaler (DPI) formulation comprising curcumin-loaded mesoporous polydopamine nanoparticles (CMPN) for the prevention and treatment of RP.<sup>114</sup> Both curcumin and polydopamine possess intrinsic antioxidant and radical-scavenging activities, which act synergistically in CMPN to mitigate oxidative stress by eliminating ROS. Additionally, CMPN enhances superoxide dismutase (SOD) activity, inhibits lipid peroxidation (eg, by reducing malondialdehyde [MDA] levels), and suppresses the release of pro-inflammatory cytokines.

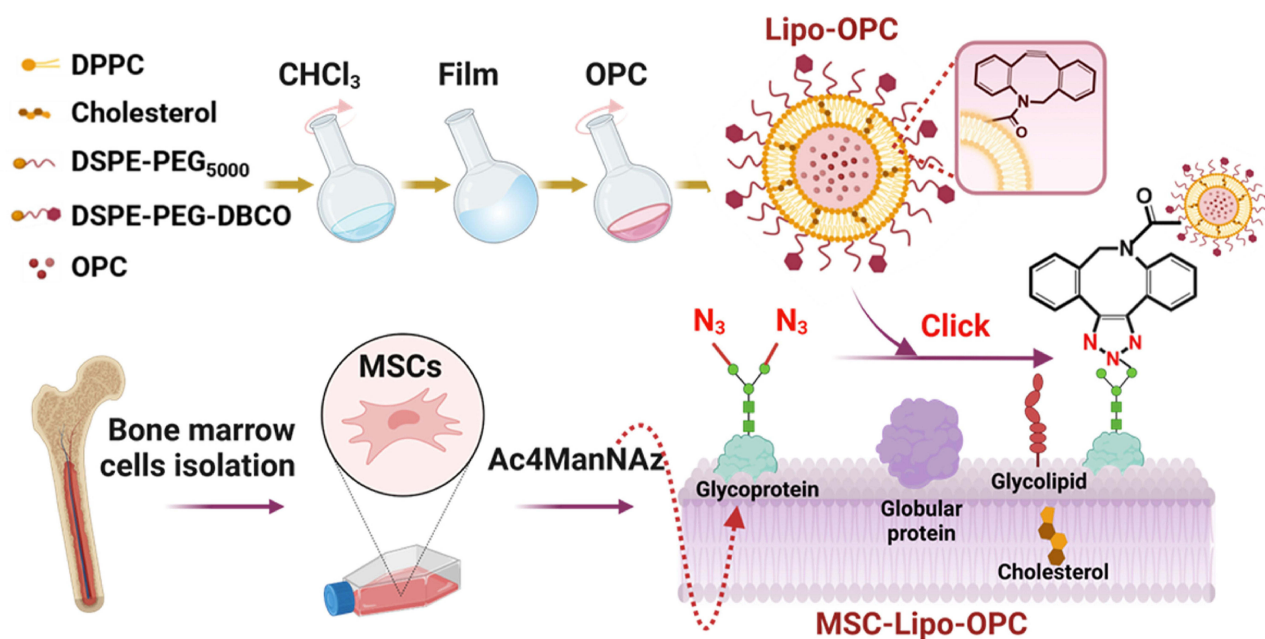
The mesoporous polydopamine (MPDA) structure offers a high drug-loading capacity and surface area, allowing for a curcumin loading efficiency of up to 47%. In CMPN, curcumin is maintained in an amorphous state, resulting in significantly improved dissolution and accelerated release, with over 80% cumulative release within 6 hours. The adhesive nature of PDA facilitates the aggregation of CMPN into microparticles in dry powder form. The formulation exhibits a mass median aerodynamic diameter (MMAD) of  $5.17 \pm 0.04 \mu\text{m}$ —smaller than that of solid particles with the same geometric diameter—favoring pulmonary deposition (lung deposition rate: 29.8%) and minimizing alveolar macrophage uptake. In a murine model of moderate RP induced by a single 15 Gy thoracic irradiation, pulmonary assessments at day 28 post-irradiation revealed that CMPN inhalation significantly reduced pulmonary hemorrhage and fibrosis compared to the untreated model group. Notably, CMPN-treated animals showed no hemorrhage, reduced inflammatory cell infiltration, and preserved alveolar architecture, demonstrating superior efficacy over dexamethasone, a positive control.<sup>114</sup>

## Cell–Nanoparticle Hybrid Systems

Cell–nanoparticle hybrid systems represent a novel therapeutic platform that integrates the biological functions of living cells with the versatile delivery capabilities of nanocarriers. Central to this approach is the synergistic combination of cell-mediated biological activity and the targeting, protective, and sustained-release properties conferred by nanomaterials. Such systems have demonstrated substantial promise in regenerative medicine and tissue engineering, particularly in the management of inflammation-associated disorders and radiation-induced tissue damage.

Mesenchymal stem cells (MSCs) have been widely studied for their immunomodulatory properties; however, their therapeutic efficacy remains limited in inflammatory diseases, partly due to poor drug delivery to pathological sites. To address this limitation, Zhou et al developed a hybrid construct wherein antioxidant-loaded liposomes (Lipo-OPC, Figure 6) were conjugated onto the surface of MSCs via click chemistry, yielding a membrane-anchored nanotherapeutic termed MSC-Lipo-OPC.<sup>115</sup> Significantly, this surface functionalization did not compromise MSC viability, inflammatory response profile, or proangiogenic capacity. In a murine model of X-ray-induced RP, intravenously administered MSC-Lipo-OPC demonstrated targeted accumulation in inflamed lung tissues. This targeting was facilitated by the micron-scale size of MSCs and their innate tropism toward inflammatory microenvironments, enabling prolonged retention within the irradiated pulmonary lesions. Mechanistically, therapeutic benefits of MSC-Lipo-OPC were attributed to three primary effects: (i) attenuation of oxidative stress via the ROS-scavenging capability of Lipo-OPC; (ii) modulation of the immune microenvironment, including reduced neutrophil infiltration, polarization of macrophages toward the anti-inflammatory M2 phenotype, and increased recruitment of regulatory T cells; and (iii) enhanced tissue regeneration through upregulation of reparative cytokines such as IL-10 and VEGF, which suppressed inflammation and promoted angiogenesis. Collectively, this membrane-anchoring strategy for nanoparticle functionalization of MSCs enables co-delivery of stem cells and therapeutic agents, significantly augmenting their therapeutic performance against radiation-induced pulmonary injury. This study thus provides a compelling framework for enhancing the clinical utility of MSCs in radioprotection, offering a promising avenue for the treatment of radiation-induced pneumonitis and pulmonary fibrosis.

To better summarize the diverse nanomedicine strategies for RILI and their key characteristics, Table 6 provides a systematic classification and comparison of these systems. It covers various categories, including polymeric carriers



## Radiation-induced lung injury (RILI)

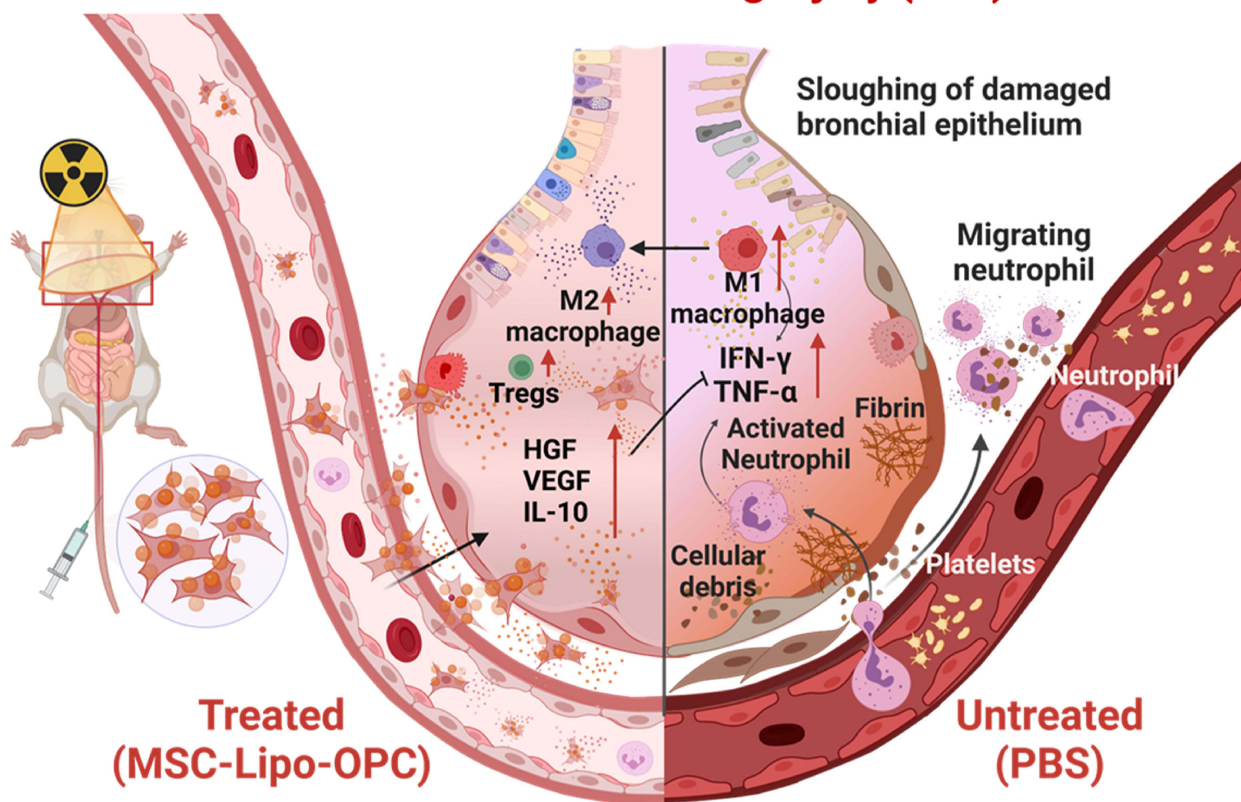


**Figure 6** The schematic illustration of MSC-Lipo-OPC-mediated radiation lung injury repair. DSPE-PEG-DBCO could be modified on OPC-loaded liposomes, and Ac4ManNAz could be exposed on the membrane surface of Ac4ManNAz-treated MSCs. MSC-Lipo-OPC was obtained through a click chemical reaction between DBCO-Lipo-OPC and Ac4ManNAz-treated MSCs. Moreover, MSC-Lipo-OPC targeted to the X-ray-exposed lungs and effectively relieved radiation pneumonia/fibrosis via regulating anti-inflammatory immune responses. Used from Zhou H, Zhang Y, Pei P, et al. Liposome-anchored mesenchymal stem cells for radiation pneumonia/fibrosis treatment. *Biomaterials*. 2023; 300: 122202. Permission conveyed through Copyright Clearance Centre, Inc.

**Table 6** Classification and Mechanisms of Nanomedicine Strategies for RILI

Category		System	Mechanism of Action	Administration	Key Outcomes	Data Source Type	Ref
Polymeric Carriers	Synthetic polymers	PLGA microspheres (Rosmarinic acid)	Mechanical lung entrapment; M2 macrophage polarization inhibition; TGF- $\beta$ 1/ $\alpha$ -SMA downregulation	Inhalation	Fibrotic area $\downarrow$ 40%; Inspiratory capacity $\uparrow$ 57.8%	Animal experiment (mouse model of pulmonary fibrosis induced by 15 Gy chest irradiation)	[97,98]
		PLGA nanoparticles (Melatonin)	miR-21/TGF- $\beta$ 1/Smad3 axis modulation; Alveolar epithelial apoptosis suppression	Intratracheal	Caspase-3 activity $\downarrow$ 35%	Animal experiment (radiation-induced lung injury rat model)	[99]
	Natural polymers	Chitosan-based hydrogel	$\uparrow$ Antioxidant enzymes (SOD: 52 IU/mL; GPx: 37 IU/mL); MDA reduction	Intraperitoneal	Alveolar wall thickness $\downarrow$ 60%; Collagen $\downarrow$ 50%	Animal experiment (15 Gy radiation treatment rat model, observation period of 50 days)	[100]
		Hyaluronic acid nanoparticles (HANPs)	TGF- $\beta$ 1/MMP-2/9 modulation; Redox homeostasis	–	Anti-inflammatory /antifibrotic effects	Animal experiment (mouse lung injury model with unclear radiation dose)	[93]
	Bioengineered Nanoreactors	SOD@ARA290-HBc	Acts by protecting alveolar epithelial cell integrity, inhibiting oxidative stress, reducing inflammatory responses, and regulating immune responses	Intratracheal administration	Improves acute radiation pneumonitis and pulmonary fibrosis, enhances SOD stability, and prolongs ARA290 half-life	Animal experiment (radiation-induced lung injury mouse model)	[101]
	Polymer-microalgae hybrid	SP@ASXnano (Spirulina-Astaxanthin NPs)	ROS scavenging; Gut microbiota modulation ( $\uparrow$ Akkermansia); $\uparrow$ SCFAs (butyrate 2.5 $\times$ )	Oral	Median survival $\uparrow$ (11.5 $\rightarrow$ 29 d); Intestinal ROS $\downarrow$ 45%; Leukocytes/platelets $\uparrow$ 30%	Animal experiment (10 Gy whole-body irradiation mouse model)	[91]

<b>Inorganic Carriers</b>	Hafnium oxide (HfO <sub>2</sub> NPs)	Size-tuned (122.9 nm lung-targeted)	SOD/CAT/GPx mimetic activity; FoxO/Hippo/TNF pathway inhibition	IV injection	γ-H2AX foci ↓60%; Lung SOD ↑2x; Survival ↑78%	Animal experiment (20 Gy whole-body irradiation rabbit model)	[92]
	Cerium oxide (CeO <sub>2</sub> NPs)	PEGylated CeO <sub>2</sub> -miR-146a	Ce <sup>3+</sup> /Ce <sup>4+</sup> redox cycling (ROS scavenging); miR-146a-mediated TLR4/NF-κB inhibition	Inhalation	Inflamed area ↓55%; Neutrophil infiltration ↓45%	Animal experiment (15 Gy radiation-induced acute lung injury mouse model, treatment period of 7 days)	[102]
	Advanced Composite Nanoplatforms	NPs Ce(phen)Pirf <sub>3</sub>	Reduces fibrotic collagen deposition; regulates EMT markers (modulates α-SMA, TGF-β1, E-cadherin, N-cadherin)	–	Improves lung function, alleviates radiation-induced lung pathology, and inhibits RIPP progression	Animal experiment (mouse model of pulmonary fibrosis with unclear radiation dose)	[103]
<b>Stimuli-Responsive</b>	ROS-responsive	CS-PBA-Cro microspheres	PBA ester cleavage (H <sub>2</sub> O <sub>2</sub> >100 μM); Passive lung targeting	Inhalation	MDA ↓40%; Alveolar wall thickness ↓25%	Animal experiment (20 Gy radiation treatment, mouse model, observation period of 7 days)	[105]
	pH-responsive	RP@BDC microspheres (Res/siPAI-I co-delivery)	CaCO <sub>3</sub> shell dissolution (pH 6.2); Anti-inflammatory/antifibrotic release	Inhalation	Spatiotemporal targeting of inflammation/fibrosis	Animal experiment (mouse model of lung injury with unclear radiation dose)	[106]
	Biological Signal-Responsive Targeted Systems	LET-bFGF	LET peptide targets damaged pulmonary endothelial cells, enriching bFGF at injury sites	Intravenous administration (25nmol/kg)	Enhances targeting to damaged lung tissue, reduces endothelial cell apoptosis, and fibrosis-related pathological changes	Animal experiment (15 Gy chest irradiation rat model, observation period of 2 months)	[107]
<b>Nucleic Acid Delivery</b>	CRISPR/Cas9	Ad-CRISPR-TGF-β1 (Adenoviral)	TGFβ1 gene editing; CTGF/α-SMA suppression	IV injection	Fibrosis attenuation	Animal experiment (radiation-induced pulmonary fibrosis mouse model)	[109]
	miRNA carrier	CeO <sub>2</sub> -miR-146a	TLR4/NF-κB pathway inhibition; ROS clearance	Intratracheal	Anti-inflammatory /antioxidant effects	Animal experiment (Bolaimycin-induced acute lung injury mouse model, indirectly derived, applicable to RILI)	[102]

(Continued)

Table 6 (Continued).

Category	System	Mechanism of Action	Administration	Key Outcomes	Data Source Type	Ref	
<b>Inhalable Nanomedicines</b>	Nanogels	Alginate nanogels (Quercetin)	Mucus penetration; NLRP3 inflammasome inhibition; Tight junction protein upregulation	Aerosol inhalation	Protein extravasation ↓50%; Edema ↓60%	Animal experiment (paraquat-induced acute lung injury rat model, indirectly derived for RILI)	[110]
	Nanosuspensions	Tetrandrine-hydroxypropyl-β-cyclodextrin inclusion complex nanosuspension	Exerts anti-inflammatory and antifibrotic effects	Inhalation administration	Improves solubility and uptake efficiency, increases survival rate in bleomycin-induced pulmonary fibrosis models	Animal experiment (Bolamycin-induced pulmonary fibrosis mouse model, indirectly derived for RILI)	[111,112]
	Nanosuspensions	BIO 300 (genistein nanosuspension)	Enhances solubility and bioavailability, targets lung tissue, inhibits oxidative stress and related cytokines	Oral administration (400mg/kg)	Improves the survival rate of irradiated mice, enhances lung function, and reduces fibrosis and inflammatory damage	Animal experiment (11.0 Gy or 12.5 Gy full chest irradiation C57L/J mouse model, administration period 4–6 weeks)	[113]
	Dry powder inhaler (DPI)	CMPN (Curcumin-mesoporous PDA NPs)	Synergistic ROS scavenging; SOD ↑; MDA ↓; Anti-cytokine effects	Inhalation	↓Hemorrhage/fibrosis; Alveolar preservation (outperforms dexamethasone)	Animal experiment (15 Gy single chest irradiation induced moderate pneumonia in a mouse model, observation period of 28 days)	[112]
<b>Cell-Nanoparticle Hybrid</b>	MSC-liposome conjugate	MSC-Lipo-OPC	MSC inflammatory tropism; Liposomal ROS scavenging; M2 macrophage polarization	IV injection	↓Neutrophil infiltration; Tissue regeneration (↑IL-10/VEGF)	Animal experiment (X-ray induced radiation-induced pneumonia mouse model)	[115]

(synthetic, natural, and polymer-microalgae hybrids), inorganic carriers, stimuli-responsive systems, nucleic acid delivery platforms, inhalable nanomedicines, and cell-nanoparticle hybrid systems. For each system, the table details its mechanism of action, administration route, and key outcomes, offering a concise overview of the advancements in nanomedicine-based drug delivery for RILI treatment.

## Challenges and Future Directions

Although NDDSs offer considerable therapeutic potential for the management of RILI, several critical challenges continue to hinder their clinical translation. One major limitation pertains to biosafety, particularly the unintended accumulation of nanoparticles in non-target organs. For instance, ultrasmall hafnium oxide nanoparticles (HfO<sub>2</sub> NPs; ~2.4 nm) have been shown to preferentially localize in the liver and kidneys, raising concerns regarding off-target toxicity, immune system activation, and potential metal ion-mediated cytotoxicity. In parallel, the complex manufacturing processes associated with advanced NDDS platforms—such as microalgae-nanoparticle hybrids or multi-stimuli-responsive microspheres—contribute to batch-to-batch variability, posing substantial barriers to standardization, reproducibility, and Good Manufacturing Practice (GMP)-compliant large-scale production.

To facilitate the clinical advancement of NDDSs for RILI, future research efforts should prioritize several strategic directions. First, the rational design of multifunctional nanoplatforms capable of simultaneously exerting antioxidant, anti-inflammatory, and anti-fibrotic activities is essential to address the multifactorial nature of RILI pathogenesis. Second, the integration of artificial intelligence (AI)-driven approaches to optimize key nanoparticle parameters—such as size, surface properties, and ligand density—based on patient-specific factors (eg, disease stage, molecular biomarkers, and radiomic features) may enhance targeting specificity, therapeutic efficacy, and safety. For instance, AI models trained on patient-derived organoid data can predict the cellular uptake efficiency of NDDS in irradiated alveolar epithelial cells, enabling the design of patient-tailored carrier surfaces. Additionally, deep learning algorithms can analyze longitudinal imaging data to forecast the progression rate of lung fibrosis, thus optimizing the release kinetics of anti-fibrotic agents in stimulus-responsive NDDS. Third, the development of more stable and durable cell-nanoparticle hybrid systems, including strategies to improve the anchoring and longevity of liposomes on mesenchymal stem cells (MSCs), could significantly enhance active targeting and co-delivery efficiency. Lastly, the incorporation of theranostic functionalities—such as embedding imaging agents (eg, HfO<sub>2</sub> NPs) within the delivery system for computed tomography (CT)—offers a promising pathway toward real-time monitoring of biodistribution, pharmacokinetics, and therapeutic responses. Such image-guided, personalized nanomedicine approaches may ultimately enable precision therapy for patients with RILI.

In the field of nanomedicine for RILI, although preclinical studies have demonstrated promising therapeutic potential, current findings remain inconsistent and face substantial challenges in clinical translation. For example, the lung-targeting efficiency of commonly used nanocarriers, such as PLGA, varies considerably depending on surface modifications, animal models, and experimental conditions.<sup>116</sup> Similarly, the therapeutic performance of ROS-responsive NDDS is dose-dependent and influenced by drug metabolism and carrier degradation, leading to a delicate balance between short-term efficacy and long-term safety risks. Moreover, the immunomodulatory effects of cell-nanoparticle hybrid systems are highly context-dependent, being influenced by the baseline immune microenvironment of the disease model. Additional concerns include biosafety issues, as nanocarriers may accumulate in non-target tissues or induce immunogenicity, while degradation products of biodegradable carriers may exert adverse biological effects. Furthermore, discrepancies between animal models and human physiology in pathophysiology, pharmacokinetics, and pharmacodynamics pose significant translational barriers. Beyond these biological challenges, technical and regulatory obstacles—including large-scale manufacturing, quality control, and standardized evaluation systems—remain major hurdles that must be addressed before successful clinical application.

## Conclusions and Outlook

NDDS for RILI have shown promising potential, yet several key challenges hinder their clinical translation. These challenges fall into three interconnected domains. First, biosafety concerns remain critical, as nanocarriers may accumulate in non-target organs and cause unexpected toxicity.<sup>117</sup> Second, translational gaps persist between preclinical and clinical outcomes, owing to species-specific differences in pathophysiology, pharmacokinetics, and

pharmacodynamics, which limit reproducibility in humans. Third, technological hurdles—particularly the complexity of advanced platforms such as multi-stimuli-responsive microspheres and cell–nano hybrids—complicate large-scale production, batch consistency, and compliance with Good Manufacturing Practice (GMP).

Despite these obstacles, major opportunities for innovation are emerging. Multifunctional nanoplatfoms can integrate antioxidant, anti-inflammatory, and antifibrotic properties into a single carrier to match the multifaceted pathology of RILI. AI-driven personalization allows dynamic adjustment of particle size, ligand density, and release kinetics based on patient-specific data, including radiation dose, radiomics, and biomarker profiles. Theranostic integration further combines diagnostic and therapeutic functions—such as HfO<sub>2</sub> nanoparticle-based CT imaging—with drug delivery, enabling real-time monitoring of biodistribution and treatment efficacy. Together, these directions provide a pathway to overcome current bottlenecks and accelerate clinical translation.

RILI, encompassing both RP and RILF, continues to be a major obstacle in thoracic radiotherapy. Its pathogenesis is driven by radiation-induced oxidative stress and DNA damage, followed by aberrant tissue repair and immune dysregulation, including TGF- $\beta$  overexpression and Th1/Th2 imbalance. Existing diagnostic and therapeutic strategies remain limited by delayed detection and suboptimal efficacy. NDDS offers a transformative platform to address these gaps by enhancing the therapeutic performance of natural biomolecules (eg, hyaluronic acid) and bioactive compounds (eg, curcumin, astaxanthin), or by engineering intelligent carriers such as ROS-responsive microspheres, inhalable nanoparticles, and exosomes. These systems enable targeted delivery, stimulus-responsive release, and reduced systemic toxicity, while simultaneously modulating multiple pathological features—oxidative stress, inflammation, fibrosis, and gene dysregulation—that underlie RILI progression.

Looking ahead, several priorities must be addressed to facilitate successful translation: (1) elucidating the interactions between nanocarriers and the pulmonary microenvironment, including immune cells and extracellular matrix; (2) optimizing biosafety, biodegradability, and large-scale GMP production; (3) advancing intelligent, multi-stimuli-responsive designs for precise spatiotemporal drug release; and (4) integrating AI and radiomics into nano-diagnostic platforms for individualized prediction, early intervention, and real-time monitoring.

Through interdisciplinary collaboration spanning nanotechnology, pharmaceutical sciences, immunology, radiobiology, imaging, and AI, NDDS holds strong promise to provide safer, more precise, and more effective interventions for RILI. Ultimately, such advances could not only improve patient outcomes following thoracic radiotherapy but also establish a framework for nanomedicine-based management of other radiation-related disorders.

## Abbreviations

3D-CRT, three-dimensional conformal radiotherapy; AI, artificial intelligence; ALI, acute lung injury; ARDS, acute respiratory distress syndrome; CAT, catalase; CeO<sub>2</sub> NPs, cerium oxide nanoparticles; CT, computed tomography; CTCAE, Common Terminology Criteria for Adverse Events; DAMPs, damage-associated molecular patterns; DLCO, diffusion capacity for carbon monoxide; DPPC, dipalmitoylphosphatidylcholine; DPIs, dry powder inhalers; ECM, extracellular matrix; EMT, epithelial-mesenchymal transition; FDA, Food and Drug Administration; FRC, functional residual capacity; FVC, forced vital capacity; GPx, glutathione peroxidase; GRP, gastrin-releasing peptide; Gy, Gray (radiation dose unit); HA, hyaluronic acid; HANPs, hyaluronic acid nanoparticles; HfO<sub>2</sub> NPs, hafnium oxide nanoparticles; HRCT, high-resolution computed tomography; ICAM-1, intercellular adhesion molecule-1; ICIs, immune checkpoint inhibitors; IFN- $\gamma$ , interferon gamma; IL, interleukin; IMRT, intensity-modulated radiotherapy; MDA, malondialdehyde; MET, melatonin; MSCs, mesenchymal stem cells; mtDNA, mitochondrial DNA; NDDS, nanodrug delivery system; NHEJ, non-homologous end joining; NK, natural killer; PECAM-1, platelet endothelial cell adhesion molecule-1; PLGA, poly(lactic-co-glycolic acid); RA, rosmarinic acid; RILI, radiation-induced lung injury; RILF, radiation-induced lung fibrosis; RNS, reactive nitrogen species; ROS, reactive oxygen species; RP, radiation pneumonitis; RV, residual volume; SBRT, stereotactic body radiotherapy; siRNA, small interfering RNA; SOD, superoxide dismutase; SSBs, single-strand breaks; TBLB, transbronchial lung biopsy; TCM, traditional Chinese medicine; TGF- $\beta$ , transforming growth factor beta; Th, T helper; TNF- $\alpha$ , tumor necrosis factor alpha; Tregs, regulatory T cells; VATS, video-assisted thoracoscopic surgery; VC, vital capacity; VMAT, volumetric modulated arc therapy; RA, Rosmarinic

Acid; MET, Melatonin; QU, Quercetin; Res, Resveratrol; Cro, Crocin; OPC, Oligomeric Proanthocyanidins; MS, Microspheres; MPDA, Mesoporous Polydopamine.

## Data Sharing Statement

Data sharing is not applicable to this article as no new data were created or analyzed in this study.

## Author Contributions

All authors made a significant contribution to the work reported, whether that is in the conception, study design, execution, acquisition of data, analysis and interpretation, or in all these areas; took part in drafting, revising or critically reviewing the article; gave final approval of the version to be published; have agreed on the journal to which the article has been submitted; and agree to be accountable for all aspects of the work.

## Funding

This research was supported by Zhejiang Provincial Natural Science Foundation of China under Grant No. LTGD24H220001 and LQ24H300001; National Natural Science Foundation of China (32401196), Natural Science Foundation of Hangzhou (2024SZRYBH090001); Natural Science Foundation of Jiangsu Province for Universities (24KJB350011); Natural Science Foundation Project of Taizhou Science and Technology Support Programme (Social Development) (TS202402); Qinglan Project of Jiangsu Province of China (2024); The supported disciplines of Huzhou Central Hospital under Grant No KY-FCXK-20231101; Zhejiang Province First Batch of “Small yet Strong” Clinical Innovation Team Project; Zhejiang Provincial “Jianbing” and “Lingyan” R & D Program (No.2024C03174); and the Innovation Training Program for College Students in Jiangsu Province (202512917007 and 202512917009).

## Disclosure

The authors report no conflicts of interest in this work.

## References

- Arroyo-Hernández M, Maldonado F, Lozano-Ruiz F, Muñoz-Montaño W, Nuñez-Baez M, Arrieta O. Radiation-induced lung injury: current evidence. *BMC Pulm Med.* 2021;21(1):9. doi:10.1186/s12890-020-01376-4
- Lierova A, Jelicova M, Nemcova M, et al. Cytokines and radiation-induced pulmonary injuries. *J Radiat Res.* 2018;59(6):709–753. doi:10.1093/jrr/rry067
- Hanania AN, Mainwaring W, Ghebre YT, Hanania NA, Ludwig M. Radiation-Induced Lung Injury: assessment and Management. *Chest.* 2019;156(1):150–162. doi:10.1016/j.chest.2019.03.033
- Wang Y, Zhang J, Shao C. Cytological changes in radiation-induced lung injury. *Life Sci.* 2024;358:123188. doi:10.1016/j.lfs.2024.123188
- Wang Y, Yu J, Ghosh T, Mayassi N. Beyond the target: a review of radiation-induced bystander effects in radiobiology and radiation therapy. 2025.
- Savin IA, Zenkova MA, Sen'kova AV. Pulmonary fibrosis as a result of acute lung inflammation: molecular mechanisms, relevant in vivo models, prognostic and therapeutic approaches. *Int J Mol Sci.* 2022;23(23). doi:10.3390/ijms232314959
- Rancati T, Ceresoli GL, Gagliardi G, Schipani S, Cattaneo GM. Factors predicting radiation pneumonitis in lung cancer patients: a retrospective study. *Radiother Oncol.* 2003;67(3):275–283. doi:10.1016/s0167-8140(03)00119-1
- Madani I, De Ruyck K, Goeminne H, De Neve W, Thierens H, Van Meerbeeck J. Predicting risk of radiation-induced lung injury. *J Thorac Oncol.* 2007;2(9):864–874. doi:10.1097/JTO.0b013e318145b2c6
- Lucia F, Rehn M, Blanc-Béguin F, Le Roux PY. Radiation therapy planning of thoracic tumors: a review of challenges associated with lung toxicities and potential perspectives of gallium-68 lung PET/CT imaging. *Front Med.* 2021;8:723748. doi:10.3389/fmed.2021.723748
- Chen C, Zeng B, Xue D, et al. Pirfenidone for the prevention of radiation-induced lung injury in patients with locally advanced oesophageal squamous cell carcinoma: a protocol for a randomised controlled trial. *BMJ Open.* 2022;12(10):e060619. doi:10.1136/bmjopen-2021-060619
- Chang S, Lv J, Wang X, et al. Pathogenic mechanisms and latest therapeutic approaches for radiation-induced lung injury: a narrative review. *Crit Rev Oncol Hematol.* 2024;202:104461. doi:10.1016/j.critrevonc.2024.104461
- Chang JY, Senan S, Paul MA, et al. Stereotactic ablative radiotherapy versus lobectomy for operable stage I non-small-cell lung cancer: a pooled analysis of two randomised trials. *Lancet Oncol.* 2015;16(6):630–637. doi:10.1016/s1470-2045(15)70168-3
- Keffer S, Guy CL, Weiss E. Fatal radiation pneumonitis: literature review and case series. *Adv Radiat Oncol.* 2020;5(2):238–249. doi:10.1016/j.adro.2019.08.010
- Raza A, Rasheed T, Nabeel F, Hayat U, Bilal M, Iqbal HMN. Endogenous and exogenous stimuli-responsive drug delivery systems for programmed site-specific release. *Molecules.* 2019;24(6):1117. doi:10.3390/molecules24061117
- Liu J, Li S, Wang J, Li N, Zhou J, Chen H. Application of Nano Drug Delivery System (NDDS) in cancer therapy: a perspective. *Recent Pat Anticancer Drug Discov.* 2022;18(2):125–132. doi:10.2174/1574892817666220713150521

16. Jaffray DA, Gospodarowicz MK. Radiation Therapy for Cancer. In: Gelband H, Jha P, Sankaranarayanan R, Horton S, editors. *Cancer: Disease Control Priorities, Third Edition (Volume 3)*. The International Bank for Reconstruction and Development / The World Bank; 2015.
17. Giridhar P, Mallick S, Rath GK, Julka PK. Radiation induced lung injury: prediction, assessment and management. *Asian Pac J Cancer Prev*. 2015;16(7):2613–2617. doi:10.7314/apjcp.2015.16.7.2613
18. Yan Y, Fu J, Kowalchuk RO, et al. Exploration of radiation-induced lung injury, from mechanism to treatment: a narrative review. *Transl Lung Cancer Res*. 2022;11(2):307–322. doi:10.21037/tlcr-22-108
19. Zhao X, Shao C. Radiotherapy-mediated immunomodulation and anti-tumor abscopal effect combining immune checkpoint blockade. *Cancers*. 2020;12(10):2762. doi:10.3390/cancers12102762
20. Guo S, Yao Y, Tang Y, et al. Radiation-induced tumor immune microenvironments and potential targets for combination therapy. *Signal Transduct Target Ther*. 2023;8(1):205. doi:10.1038/s41392-023-01462-z
21. Filomeni G, De Zio D, Cecconi F. Oxidative stress and autophagy: the clash between damage and metabolic needs. *Cell Death Differ*. 2015;22(3):377–388. doi:10.1038/cdd.2014.150
22. Mandal M, Sarkar M, Khan A, et al. Reactive Oxygen Species (ROS) and Reactive Nitrogen Species (RNS) in plants— maintenance of structural individuality and functional blend. *Adv Redox Res*. 2022;5:100039. doi:10.1016/j.arres.2022.100039
23. Phaniendra A, Jestadi DB, Periyasamy L. Free radicals: properties, sources, targets, and their implication in various diseases. *Indian J Clin Biochem*. 2015;30(1):11–26. doi:10.1007/s12291-014-0446-0
24. Giuranno L, Lent J, De Ruyscher D, Vooijs MA. Radiation-induced lung injury (RILI). *Front Oncol*. 2019;9:877. doi:10.3389/fonc.2019.00877
25. Moloney JN, Cotter TG. ROS signalling in the biology of cancer. *Semin Cell Dev Biol*. 2018;80:50–64. doi:10.1016/j.semcdb.2017.05.023
26. Weber A, Wasiliew P, Kracht M. Interleukin-1 (IL-1) pathway. *Sci Signaling*. 2010;3(105):cm1. doi:10.1126/scisignal.3105cm1
27. Bonner JC. Regulation of PDGF and its receptors in fibrotic diseases. *Cytokine Growth Factor Rev*. 2004;15(4):255–273. doi:10.1016/j.cytogfr.2004.03.006
28. McCartney-Francis NL, Frazier-Jessen M, Wahl SM. TGF-beta: a balancing act. *Int Rev Immunol*. 1998;16(5–6):553–580. doi:10.3109/08830189809043009
29. Santivasi WL, Xia F. Ionizing radiation-induced DNA damage, response, and repair. *Antioxid Redox Signaling*. 2014;21(2):251–259. doi:10.1089/ars.2013.5668
30. Saini S, Gurung P. A comprehensive review of sensors of radiation-induced damage, radiation-induced proximal events, and cell death. *Immunol Rev*. 2025;329(1):e13409. doi:10.1111/imr.13409
31. Cheung EC, Vousden KH. The role of ROS in tumour development and progression. *Nat Rev Cancer*. 2022;22(5):280–297. doi:10.1038/s41568-021-00435-0
32. Srinivas US, Tan BWQ, Vellayappan BA, Jeyasekharan AD. ROS and the DNA damage response in cancer. *Redox Biol*. 2019;25:101084. doi:10.1016/j.redox.2018.101084
33. Wirsdörfer F, Cappuccini F, Niazman M, et al. Thorax irradiation triggers a local and systemic accumulation of immunosuppressive CD4+ FoxP3+ regulatory T cells. *Radiat Oncol*. 2014;9:98. doi:10.1186/1748-717x-9-98
34. Cappuccini F, Eldh T, Bruder D, et al. New insights into the molecular pathology of radiation-induced pneumopathy. *Radiother Oncol*. 2011;101(1):86–92. doi:10.1016/j.radonc.2011.05.064
35. Paun A, Kunwar A, Haston CK. Acute adaptive immune response correlates with late radiation-induced pulmonary fibrosis in mice. *Radiat Oncol*. 2015;10:45. doi:10.1186/s13014-015-0359-y
36. Sheikholeslami S, Aryafar T, Abedi-Firouzjah R, et al. The role of melatonin on radiation-induced pneumonitis and lung fibrosis: a systematic review. *Life Sci*. 2021;281:119721. doi:10.1016/j.lfs.2021.119721
37. Briukhovetska D, Dörr J, Endres S, Libby P, Dinarello CA, Kobold S. Interleukins in cancer: from biology to therapy. *Nat Rev Cancer*. 2021;21(8):481–499. doi:10.1038/s41568-021-00363-z
38. Vargas-ángel CA, Trujillo-Cirilo L, Sierra-Mondragón E, Rangel-Corona R, Weiss-Steider B. Cationic liposomes encapsulating IL-2 selectively induce apoptosis and significantly reduce the secretion of cytokines on M1-murine polarized macrophages. *Cytokine*. 2025;189:156903. doi:10.1016/j.cyto.2025.156903
39. Sandler NG, Mentink-Kane MM, Cheever AW, Wynn TA. Global gene expression profiles during acute pathogen-induced pulmonary inflammation reveal divergent roles for Th1 and Th2 responses in tissue repair. *J Immunol*. 2003;171(7):3655–3667. doi:10.4049/jimmunol.171.7.3655
40. Hoffmann KF, McCarty TC, Segal DH, et al. Disease fingerprinting with cDNA microarrays reveals distinct gene expression profiles in lethal type 1 and type 2 cytokine-mediated inflammatory reactions. *FASEB J*. 2001;15(13):2545–2547. doi:10.1096/fj.01-0306fje
41. Zhao B, Yu X, Shi J, et al. A stepwise mode of TGFβ-SMAD signaling and DNA methylation regulates naïve-to-primed pluripotency and differentiation. *Nat Commun*. 2024;15(1):10123. doi:10.1038/s41467-024-54433-5
42. Huehn J, Siegmund K, Lehmann JC, et al. Developmental stage, phenotype, and migration distinguish naive- and effector/memory-like CD4+ regulatory T cells. *J Exp Med*. 2004;199(3):303–313. doi:10.1084/jem.20031562
43. Sheng Y, Chen K, Jiang W, et al. PD-1 restrains IL-17A production from γδ T cells to modulate acute radiation-induced lung injury. *Transl Lung Cancer Res*. 2021;10(2):685–698. doi:10.21037/tlcr-20-838
44. Xiong S, Pan X, Xu L, et al. Regulatory T cells promote β-catenin-mediated epithelium-to-mesenchyme transition during radiation-induced pulmonary fibrosis. *Int J Radiat Oncol Biol Phys*. 2015;93(2):425–435. doi:10.1016/j.ijrobp.2015.05.043
45. Xiong S, Guo R, Yang Z, et al. Treg depletion attenuates irradiation-induced pulmonary fibrosis by reducing fibrocyte accumulation, inducing Th17 response, and shifting IFN-γ, IL-12/IL-4, IL-5 balance. *Immunobiology*. 2015;220(11):1284–1291. doi:10.1016/j.imbio.2015.07.001
46. Wang P, Yan Z, Zhou PK, Gu Y. The promising therapeutic approaches for radiation-induced pulmonary fibrosis: targeting radiation-induced mesenchymal transition of alveolar type II epithelial cells. *Int J Mol Sci*. 2022;23(23). doi:10.3390/ijms232315014
47. Gunatilaka A, Zhang S, Tan WSD, Stewart AG. Anti-fibrotic strategies and pulmonary fibrosis. *Adv Pharmacol*. 2023;98:179–224. doi:10.1016/bs.apha.2023.04.002
48. Zhang H, Qi L, Cai Y, Gao X. Gastrin-releasing peptide receptor (GRPR) as a novel biomarker and therapeutic target in prostate cancer. *Ann Med*. 2024;56(1):2320301. doi:10.1080/07853890.2024.2320301
49. Zhou S, Nissao E, Jackson IL, et al. Radiation-induced lung injury is mitigated by blockade of gastrin-releasing peptide. *Am J Pathol*. 2013;182(4):1248–1254. doi:10.1016/j.ajpath.2012.12.024

50. Liu Y, Guo J, Liu C, et al. Unveiling pharmacological targets of Rihimaside C for radiation-induced lung injury: an in silico and experimental integrated approach. *2024*.
51. Zhou Z, Xie Y, Wei Q, Zhang X, Xu Z. Revisiting the role of MicroRNAs in the pathogenesis of idiopathic pulmonary fibrosis. *Front Cell Dev Biol.* **2024**;12:1470875. doi:10.3389/fcell.2024.1470875
52. Qin S, Tan P, Xie J, Zhou Y, Zhao J. A systematic review of the research progress of traditional Chinese medicine against pulmonary fibrosis: from a pharmacological perspective. *ChinMed.* **2023**;18(1):96. doi:10.1186/s13020-023-00797-7
53. Wang L, Li S, Yao Y, Yin W, Ye T. The role of natural products in the prevention and treatment of pulmonary fibrosis: a review. *Food Funct.* **2021**;12(3):990–1007.
54. Ikushima H, Miyazono K. TGFbeta signalling: a complex web in cancer progression. *Nat Rev Cancer.* **2010**;10(6):415–424. doi:10.1038/nrc2853
55. Guo YJ, Pan WW, Liu SB, Shen ZF, Xu Y, Hu LL. ERK/MAPK signalling pathway and tumorigenesis. *Exp Ther Med.* **2020**;19(3):1997–2007. doi:10.3892/etm.2020.8454
56. Bozyk PD, Moore BB. Prostaglandin E2 and the pathogenesis of pulmonary fibrosis. *Am J Respir Cell Mol Biol.* **2011**;45(3):445–452. doi:10.1165/rcmb.2011-0025RT
57. Ahn H, Kim JH, Lee KC, et al. Early prediction of radiation-induced pulmonary fibrosis using gastrin-releasing peptide receptor-targeted PET imaging. *Mol Pharmaceut.* **2023**;20(1):267–278. doi:10.1021/acs.molpharmaceut.2c00632
58. Roy S, Salerno KE, Citrin DE. Biology of radiation-induced lung injury. *Sem Rad Oncol.* **2021**;31(2):155–161. doi:10.1016/j.semradonc.2020.11.006
59. Ruyscher D, Wauters E, Jendrossek V, et al. Diagnosis and treatment of radiation induced pneumonitis in patients with lung cancer: an ESTRO clinical practice guideline. *Radiother Oncol.* **2025**;207:110837. doi:10.1016/j.radonc.2025.110837
60. Lumniczky K, Impens N, Armengol G, et al. Low dose ionizing radiation effects on the immune system. *Environ Int.* **2021**;149:106212. doi:10.1016/j.envint.2020.106212
61. Liu XC, Zhou PK. Tissue reactions and mechanism in cardiovascular diseases induced by radiation. *Int J Mol Sci.* **2022**;23(23). doi:10.3390/ijms232314786
62. Rahi MS, Parekh J, Pednekar P, et al. Radiation-induced lung injury-current perspectives and management. *Clin Pract.* **2021**;11(3):410–429. doi:10.3390/clinpract11030056
63. Zhou C, Yu J. Chinese expert consensus on diagnosis and treatment of radiation pneumonitis. *Precis Radiat Oncol.* **2022**;6(3):262–271.
64. Angelopoulou E, Androni X, Villa C, Hatzimanolis A, Scarneas N, Papageorgiou S. Blood-based biomarkers in mild behavioral impairment: an updated overview. *Front Neurol.* **2025**;16:1534193. doi:10.3389/fneur.2025.1534193
65. Mathew L, Evans A, Ouriadov A, et al. Hyperpolarized 3He magnetic resonance imaging of chronic obstructive pulmonary disease: reproducibility at 3.0 tesla. *Acad Radiol.* **2008**;15(10):1298–1311. doi:10.1016/j.acra.2008.04.019
66. Nissen A, Audi SH, Clough AV, et al. Advances in noninvasive imaging for detecting radiation-induced lung injury (RILI). *Int J Radiat Biol.* **2025**:1–13. doi:10.1080/09553002.2025.2531903
67. Roden AC, Camus P. Iatrogenic pulmonary lesions. *Semin Diagn Pathol.* **2018**;35(4):260–271. doi:10.1053/j.semdp.2018.03.002
68. Yan Y, Wu L, Li X, Zhao L, Xu Y. Immunomodulatory role of azithromycin: potential applications to radiation-induced lung injury. *Front Oncol.* **2023**;13:966060. doi:10.3389/fonc.2023.966060
69. Aqeel M, Medhora M, Gore E, et al. Evaluation of radiation-induced pleural effusions after radiotherapy to support development of animal models of radiation pneumonitis. *Health Phys.* **2021**;121(4):434–443. doi:10.1097/HP.0000000000001462
70. Chen Z, Wang B, Wu Z, et al. The occurrence and development of radiation-induced lung injury after interstitial brachytherapy and stereotactic radiotherapy in SD rats. *J Inflamm.* **2023**;20(1):23. doi:10.1186/s12950-023-00348-9
71. Varghese AP, Naik S, Andrabi SAUH, Luharia A, Tivaskar S. Enhancing radiological diagnosis: a comprehensive review of image quality assessment and optimization strategies. *Cureus.* **2024**;16(6):e63016. doi:10.7759/cureus.63016
72. Zhang Z, Wang Z, Luo T, et al. Computed tomography and radiation dose images-based deep-learning model for predicting radiation pneumonitis in lung cancer patients after radiation therapy. *Radiother Oncol.* **2023**;182:109581. doi:10.1016/j.radonc.2023.109581
73. Feng A, Huang Y, Zeng Y, et al. Improvement of prediction performance for radiation pneumonitis by using 3-dimensional dosiomic features. *Clin Lung Cancer.* **2024**;25(4):e173–e180.e2. doi:10.1016/j.clcc.2024.01.006
74. Thomas HMT, Hippe DS, Forouzaneshad P, et al. Radiation and immune checkpoint inhibitor-mediated pneumonitis risk stratification in patients with locally advanced non-small cell lung cancer: role of functional lung radiomics? *Discov Oncol.* **2022**;13(1):85. doi:10.1007/s12672-022-00548-4
75. Bo Z, Song J, He Q, et al. Application of artificial intelligence radiomics in the diagnosis, treatment, and prognosis of hepatocellular carcinoma. *Comput Biol Med.* **2024**;173:108337. doi:10.1016/j.compbimed.2024.108337
76. Siegel RL, Miller KD, Wagle NS, Jemal A. Cancer statistics, 2023. *CA A Cancer J Clinicians.* **2023**;73(1):17–48. doi:10.3322/caac.21763
77. Zhang J, Ge P, Liu J, et al. Glucocorticoid treatment in acute respiratory distress syndrome: an overview on mechanistic insights and clinical benefit. *Int J Mol Sci.* **2023**;24(15). doi:10.3390/ijms241512138
78. Finnerty JP, Ponnuswamy A, Dutta P, Abdelaziz A, Kamil H. Efficacy of antifibrotic drugs, nintedanib and pirfenidone, in treatment of progressive pulmonary fibrosis in both idiopathic pulmonary fibrosis (IPF) and non-IPF: a systematic review and meta-analysis. *BMC Pulm Med.* **2021**;21(1):411. doi:10.1186/s12890-021-01783-1
79. Lancaster LH, de Andrade JA, Zibrak JD, et al. Pirfenidone safety and adverse event management in idiopathic pulmonary fibrosis. *Eur Respir Rev.* **2017**;26(146):170057. doi:10.1183/16000617.0057-2017
80. Dash S, Sahu AK, Srivastava A, Chowdhury R, Mukherjee S. Exploring the extensive crosstalk between the antagonistic cytokines- TGF-β and TNF-α in regulating cancer pathogenesis. *Cytokine.* **2021**;138:155348. doi:10.1016/j.cyto.2020.155348
81. Zhu H-Z, Li C-Y, Liu L-J, et al. Efficacy and safety of Qingfei Huatan formula in the treatment of acute exacerbation of chronic obstructive pulmonary disease: a multi-centre, randomised, double-blind, placebo-controlled trial. *J Integr Med.* **2024**;22(5):561–569. doi:10.1016/j.joim.2024.07.003
82. Yang Y, Yang S, Chen M, Zhang X, Zou Y, Zhang X. Compound Astragalus and Salvia miltiorrhiza extract exerts anti-fibrosis by mediating TGF-β/Smad signaling in myofibroblasts. *J Ethnopharmacol.* **2008**;118(2):264–270. doi:10.1016/j.jep.2008.04.012
83. Pang XM, Cai HH, Zhao J, et al. Efficacy of astragalus in the treatment of radiation-induced lung injury based on traditional Chinese medicine: a systematic review and meta-analysis of 25 RCTs. *Medicine.* **2022**;101(36):e30478. doi:10.1097/md.00000000000030478

84. Shang M, Ke Y, Liu J, et al. A novel traditional Chinese medicine combination for radiation. *Radiat Med Prot.* 2024;5(1):37–42. doi:10.1016/j.radmp.2024.02.004
85. Mehrens H, Taylor P, Followill DS, Kry SF. Survey results of 3D-CRT and IMRT quality assurance practice. *J Appl Clin Med Phys.* 2020;21(7):70–76. doi:10.1002/acm2.12885
86. Nakamura N, Shikama N, Oguchi M. Intensity-modulated radiation therapy (IMRT). *Nippon Rinsho.* 2010;68(6):1035–1039.
87. Reuzé S, Schernberg A, Orlhac F, et al. Radiomics in nuclear medicine applied to radiation therapy: methods, pitfalls, and challenges. *Int J Radiat Oncol Biol Phys.* 2018;102(4):1117–1142. doi:10.1016/j.ijrobp.2018.05.022
88. Orlhac F, Nioche C, Klyuzhin I, Rahmim A, Buvat I. Radiomics in PET imaging: a practical guide for newcomers. *PET Clin.* 2021;16(4):597–612. doi:10.1016/j.cpet.2021.06.007
89. Danieli R, Milano A, Gallo S, et al. Personalized dosimetry in targeted radiation therapy: a look to methods, tools and critical aspects. *J Pers Med.* 2022;12(2):205. doi:10.3390/jpm12020205
90. Bracci S, Valeriani M, Agolli L, De Sanctis V, Maurizi Enrici R, Osti MF. Renin-angiotensin system inhibitors might help to reduce the development of symptomatic radiation pneumonitis after stereotactic body radiotherapy for lung cancer. *Clin Lung Cancer.* 2016;17(3):189–197. doi:10.1016/j.clcc.2015.08.007
91. Zhang D, He J, Cui J, et al. Oral microalgae-nano integrated system against radiation-induced injury. *ACS nano.* 2023;17(11):10560–10576. doi:10.1021/acsnano.3c01502
92. Liu D, Cao F, Xu Z, et al. Selective organ-targeting hafnium oxide nanoparticles with multienzyme-mimetic activities attenuate radiation-induced tissue damage. *Adv Mater.* 2024;36(19):2308098.
93. Lierova A, Kasparova J, Pejchal J, et al. Attenuation of Radiation-Induced Lung Injury by Hyaluronic Acid Nanoparticles. *Front Pharmacol.* 2020;11:1199. doi:10.3389/fphar.2020.01199
94. Man J, Shen Y, Song Y, Yang K, Pei P, Hu L. Biomaterials-mediated radiation-induced diseases treatment and radiation protection. *J Control Release.* 2024;370:318–338. doi:10.1016/j.jconrel.2024.04.044
95. Sahu T, Ratre YK, Chauhan S, Bhaskar LVKS, Nair MP, Verma HK. Nanotechnology based drug delivery system: current strategies and emerging therapeutic potential for medical science. *J Drug Delivery Sci Technol.* 2021;63:102487. doi:10.1016/j.jddst.2021.102487
96. Chang X, Qu F, Li C, et al. Development and therapeutic potential of GSP11 molecular glue degraders: a medicinal chemistry perspective. *Med Res Rev.* 2024;44(4):1727–1767. doi:10.1002/med.22024
97. Chen Y, Li Y, He Y, et al. Targeted lung therapy with rosmarinic acid encapsulated in PLGA microspheres for radiation-induced pulmonary fibrosis. *J Drug Delivery Sci Technol.* 2024;96:105710.
98. Agnoletti M, Rodriguez-Rodriguez C, Klodzińska SN, et al. Monosized polymeric microspheres designed for passive lung targeting: biodistribution and pharmacokinetics after intravenous administration. *ACS nano.* 2020;14(6):6693–6706. doi:10.1021/acsnano.9b09773
99. Wang S, Li J, He Y, et al. Protective effect of melatonin entrapped PLGA nanoparticles on radiation-induced lung injury through the miR-21/TGF- $\beta$ 1/Smad3 pathway. *Int J Pharm.* 2021;602:120584. doi:10.1016/j.ijpharm.2021.120584
100. Akbari Lasboo S, Eslami H, Razavi-Tousi SMT, Ansari M, Afroozan Bazghaleh A. The affinity of cellulose nanoparticle toward hydrogel based on chitosan/tragacanth for radiation protection: study of pulmonary damages on rats. *J Polym Sci.* 2024;62(19):4456–4471.
101. Liu T, Yang Q, Zheng H, et al. Multifaceted roles of a bioengineered nanoreactor in repressing radiation-induced lung injury. *Biomaterials.* 2021;277:121103. doi:10.1016/j.biomaterials.2021.121103
102. Niemiec SM, Hilton SA, Wallbank A, et al. Cerium oxide nanoparticle delivery of microRNA-146a for local treatment of acute lung injury. *Nanomedicine.* 2021;34:102388. doi:10.1016/j.nano.2021.102388
103. Lu J, Luo J, Li J, et al. Fluorescent Pirfenidone-Cerium (III) nanocomplexes protect against radiation-induced pulmonary fibrosis and inhibit tumor cell growth. *J Drug Delivery Sci Technol.* 2023;86:104651.
104. Zhou L, Zhu J, Liu Y, Zhou PK, Gu Y. Mechanisms of radiation-induced tissue damage and response. *MedComm.* 2024;5(10):e725. doi:10.1002/mco2.725
105. Wang L, Liu C, Lu W, Xu L, Kuang L, Hua D. ROS-sensitive Crocin-loaded chitosan microspheres for lung targeting and attenuation of radiation-induced lung injury. *Carbohydr Polym.* 2023;307:120628. doi:10.1016/j.carbpol.2023.120628
106. Wang X, Lin J, Yin D, et al. Inhalable multilevel responsive microspheres for radiation-induced lung injury. *Nano Res.* 2025;18(5).
107. Guan D, Mi J, Chen X, et al. Lung endothelial cell-targeted peptide-guided bFGF promotes the regeneration after radiation induced lung injury. *Biomaterials.* 2018;184:10–19. doi:10.1016/j.biomaterials.2018.08.061
108. Wong KH, Guo Z, Law M-K, Chen M. Functionalized PAMAM constructed nanosystems for biomacromolecule delivery. *Biomater Sci.* 2023;11(5):1589–1606. doi:10.1039/d2bm01677j
109. Zhen S, Qiang R, Lu J, Tuo X, Yang X, Li X. TGF- $\beta$ 1-based CRISPR/Cas9 gene therapy attenuates radiation-induced lung injury. *Curr Gene Ther.* 2022;22(1):59–65. doi:10.2174/1566523220666201230100523
110. Chen Y-B, Zhang Y-B, Wang Y-L, et al. A novel inhalable quercetin-alginate nanogel as a promising therapy for acute lung injury. *J Nanobiotechnol.* 2022;20(1):272. doi:10.1186/s12951-022-01452-3
111. Aldeeb MME, Wilar G, Suhandi C, Elamin KM, Wathoni N. Nanosuspension-based drug delivery systems for topical applications. *Int J Nanomed.* 2024;19:825–844. doi:10.2147/IJN.S447429
112. Su W, Liang Y, Meng Z, et al. Inhalation of tetrandrine-hydroxypropyl- $\beta$ -cyclodextrin inclusion complexes for pulmonary fibrosis treatment. *Mol Pharmaceut.* 2020;17(5):1596–1607. doi:10.1021/acs.molpharmaceut.0c00026
113. Jackson IL, Zodda A, Gurung G, et al. BIO 300, a nanosuspension of genistein, mitigates pneumonitis/fibrosis following high-dose radiation exposure in the C57L/J murine model. *Br J Pharmacol.* 2017;174(24):4738–4750. doi:10.1111/bph.14056
114. Chen T, Zhuang B, Huang Y, et al. Inhaled curcumin mesoporous polydopamine nanoparticles against radiation pneumonitis. *Acta Pharmaceutica Sinica B.* 2022;12(5):2522–2532. doi:10.1016/j.apsb.2021.10.027
115. Zhou H, Zhang Y, Pei P, Shen W, Yi X, Yang K. Liposome-anchored mesenchymal stem cells for radiation pneumonia/fibrosis treatment. *Biomaterials.* 2023;300:122202. doi:10.1016/j.biomaterials.2023.122202
116. Karra N, Nassar T, Ripin AN, Schwob O, Borlak J, Benita S. Antibody conjugated PLGA nanoparticles for targeted delivery of paclitaxel palmitate: efficacy and biofate in a lung cancer mouse model. *Small.* 2013;9(24):4221–4236. doi:10.1002/sml.201301417
117. Tripathi DK. *Molecular Pharmaceutics (Nano Technology & Targeted DDS)(NTDS)*. PharmaMed Press/BSP Books; 2024.

**International Journal of Nanomedicine**

**Publish your work in this journal**

The International Journal of Nanomedicine is an international, peer-reviewed journal focusing on the application of nanotechnology in diagnostics, therapeutics, and drug delivery systems throughout the biomedical field. This journal is indexed on PubMed Central, MedLine, CAS, SciSearch<sup>®</sup>, Current Contents<sup>®</sup>/Clinical Medicine, Journal Citation Reports/Science Edition, EMBase, Scopus and the Elsevier Bibliographic databases. The manuscript management system is completely online and includes a very quick and fair peer-review system, which is all easy to use. Visit <http://www.dovepress.com/testimonials.php> to read real quotes from published authors.

Submit your manuscript here: <https://www.dovepress.com/international-journal-of-nanomedicine-journal>

**Dovepress**  
Taylor & Francis Group